AD-A200 403

A TRIDENT SCHOLAR PROJECT REPORT

DTIC FILE COPY

NO. 153

"AN ENDO-ATMOSPHERIC HYPERVELOCITY INTERCEPT SYSTEM"

A Trident Scholar Project Report

DTIC
ELECTE
NOV 0 3 1988
S D
H

UNITED STATES NAVAL ACADEMY
ANNAPOLIS, MARYLAND

This document has been approved for public release and sale; its distribution is unlimited.

88 11 03 003

UNCLASSIFIED

SECURITY CLASSIFICATION OF THIS PAGE (When Data Entered)

REPORT DOCUMENTATION PAGE		READ INSTRUCTIONS BEFORE COMPLETING FORM
1. REPORT NUMBER U.S.N.A. - TSPR; no. 153 (1988)	2. GOVT ACCESSION NO.	3. RECIPIENT'S CATALOG NUMBER
4. TITLE (and Subtitle) AN ENDO-ATMOSPHERIC HYPERVELOCITY INTERCEPT SYSTEM.		5. TYPE OF REPORT & PERIOD COVERED Final 1977/88
		6. PERFORMING ORG. REPORT NUMBER
7. AUTHOR(s) Shawn L. Penrod		8. CONTRACT OR GRANT NUMBER(s)
9. PERFORMING ORGANIZATION NAME AND ADDRESS United States Naval Academy, Annapolis.		10. PROGRAM ELEMENT, PROJECT, TASK AREA & WORK UNIT NUMBERS
11. CONTROLLING OFFICE NAME AND ADDRESS United States Naval Academy, Annapolis.		12. REPORT DATE 10 June 1988
		13. NUMBER OF PAGES 113
14. MONITORING AGENCY NAME & ADDRESS(if different from Controlling Office)		15. SECURITY CLASS. (of this report)
		15a. DECLASSIFICATION/DOWNGRADING SCHEDULE

16. DISTRIBUTION STATEMENT (of this Report)

This document has been approved for public release; its distribution is UNLIMITED.

17. DISTRIBUTION STATEMENT (of the abstract entered in Block 20, if different from Report)

18. SUPPLEMENTARY NOTES

Accepted by the U.S. Trident Scholar Committee.

19. KEY WORDS (Continue on reverse side if necessary and identify by block number)

Antimissile missiles
Guided missiles
Computer simulation
Directed-Energy weapons

20. ABSTRACT (Continue on reverse side if necessary and identify by block number)

This study examines the feasibility and practicality of using clouds of hypervelocity pellets to intercept and disable a generic air target. The Directed Energy Projectile Warhead which accelerates these pellets, uses an unconventional design to attain speeds an order of magnitude above those of conventional high explosive warheads. The DEPW is fitted to a conventional intercept missile to put the target in effective range of the warhead, which

(OVER)

>then detonates, and launches the pellets very much like a hypervelocity shotgun.

An extensive three-dimensional computer simulation was developed using ACSL (Advanced Computer Simulation Language) and FORTRAN. The program models the terminal homing phase of a missile intercept to evaluate the effectiveness of different guidance laws used to align the warhead with the projected intercept point. After a favorable geometry has been achieved, the warhead is detonated and the lethality of impact between the target and hypervelocity pellet cloud is evaluated.

Overall effectiveness of this system is shown to depend on the pointing accuracy of the warhead and the firing range. No insurmountable obstacles are foreseen in developing a suitable guidance and aiming algorithm. Also a valuable tool to evaluate design options has been developed.

DTIC COPY INSPECTED 6

Accession For
NTIS GRA&I
DTIC TAB
Unannounced
Justification
By
Distribution/
Availability Codes
Dist | Special
A-1

U.S.N.A. - Trident Scholar project report; no. 153 (1988)

"AN ENDO-ATMOSPHERIC HYPERVELOCITY INTERCEPT SYSTEM"

A Trident Scholar Project Report

by

Midshipman First Class Shawn L. Penrod
Class of 1988

J.W. Watts

Advisor: Assoc. Prof. J. Watts
Co-Advisor: Assoc. Prof. R. DeMoyer
Weapons and Systems Engineering Department

Accepted for Trident Scholar Committee

Dennis F Hasson

Prof. D.F. Hasson, CHAIRPERSON

10 June 1988

DATE

USNA-1531-2

ABSTRACT

This study examines the feasibility and practicality of using clouds of hypervelocity pellets to intercept and disable a generic air target. The Directed Energy Projectile Warhead which accelerates these pellets, uses an unconventional design to attain speeds an order of magnitude above those of conventional high explosive warheads. The DEPW is fitted to a conventional intercept missile to put the target in effective range of the warhead, which then detonates, and launches the pellets very much like a hypervelocity shotgun.

An extensive three dimensional computer simulation was developed using ACSL (Advanced Computer Simulation Language) and FORTRAN. The program models the terminal homing phase of a missile intercept to evaluate the effectiveness of different guidance laws used to align the warhead with the projected intercept point. After a favorable geometry has been achieved, the warhead is detonated and the lethality of impact between the target and hypervelocity pellet cloud is evaluated.

Overall effectiveness of this system is shown to depend on the pointing accuracy of the warhead and the firing range. No insurmountable obstacles are foreseen in developing a suitable guidance and aiming algorithm. Also a valuable tool to evaluate design options has been developed.

PREFACE

This paper is written to satisfy the requirements of the United States Naval Academy's Tride Scholar Program and is the final report on this year long independent research project. I would like to acknowledge my advisors, Prof. Watts and Prof. DeMoyer, for their support and assistance throughout the year. Special recognition also goes to the Defense Systems Division (particularly Bill Saylor) at Los Alamos National Laboratory where this paper was conceived and on whose work much of this paper is based.

TABLE OF CONTENTS

I. INTRODUCTION....4
A. Purpose of Study 4
B. Hypervelocity 6
C. Method of Study 9
D. Organization of Study 10

II. DIRECTED ENERGY PROJECTILE WARHEAD....11
A. Configuration 11
B. Hypervelocity Atmospheric Effects 13
C. Lethality 19
D. Warhead Model 24

III. INTERCEPT MISSILE....27
A. Missile Configuration 27
B. Simplifying Assumptions 29
C. Coordinate Systems 32
D. Aerodynamic Transfer Function 35

IV. GUIDANCE SYSTEM....38
A. Boost Midcourse Phases 38
B. Terminal Homing Guidance 40
1. Pursuit Navigation 42
2. Lead Angle Navigation 44
3. Predictive Navigation 45
4. Proportional Navigation 48
5. Optimal Control 50
C. Sensors 51

V. RESULTS AND DISCUSSION....54

VI. SUMMARY AND CONCLUSION....60

FIGURES, TABLES, GRAPHS....62

REFERENCES....86

BIBLIOGRAPHY....87

APPENDIX A. DRAG EQUATIONS....89
APPENDIX B. MISSILE DYNAMICS....97
APPENDIX C. QUATERNIONS....99
APPENDIX D. COMPUTER SIMULATION CODE 102

I. INTRODUCTION

A. Purpose of Study

This study explores some of the practical considerations of hypervelocity technology for general endo-atmospheric intercept systems through analysis and computer simulation and specifically examines the potential of one recently proposed system employing a conventional missile and a new type of warhead. A major goal of this project was to develop a computer code capable of evaluating parameters to study design trade-offs to assist future weapon development.

Interest in hypervelocity technology has increased with the advent of the Strategic Defense Initiative which emphasizes the "non-nuclear" aspects of ballistic missile defense. Kinetic Energy Weapons, one of the two major areas of research, rely on the kinetic energy of solid projectiles impacting at great velocities to destroy or disable by battering, perforating, or as will be seen vaporizing all or part of the target. Kinetic energy, energy which is inherent in all moving bodies by virtue of their velocity, is defined as:

$$K.E. = \frac{1}{2} m V^2 \qquad (1)$$

where m is the mass of the body and V is the magnitude of

velocity or speed of the body. Destructive potential for Kinetic Energy Weapons is proportional to the amount of kinetic energy delivered to the target and varies with the mass of impacting material and to the square of the impact velocity. Thus, increasing either parameter increases the probability of kill (P_k) or the probability of target neutralization assuming that an impact occurs. The velocity, which is raised to an exponent, dominates this relationship making it possible to achieve large increases in kinetic energy with relatively small increases in velocity (see Table 2). Clearly, if one wishes to maximize kinetic energy and probability of kill while keeping the mass at some reasonable value it is necessary to maximize the velocity -- reasoning which provides both the basis and impetus for developing hypervelocity technology.

This work extrapolates the developments and predicted capabilities of hypervelocity systems currently being studied in the Strategic Defense Initiative, which are mainly exo-atmospheric or space-based, and translates them into an endo-atmospheric venue to evaluate deleterious atmospheric effects including drag and aerothermal heating for a narrow but promisingly effective range of performance. Central to this work is the examination of the Directed Energy Projectile Warhead, a new weapons concept which employs an unconventional high explosive (HE) warhead to propel a cloud of hypervelocity fragments from a

conventional intercept missile. Evaluation of this system will focus first on the viabilty and practicality of such a system and secondly on its relative effectiveness as compared to conventional intercept systems.

B. Hypervelocity

"Hypervelocity" in this paper describes speeds exceeding those readily attainable by objects within the atmosphere through the use of conventional chemical propellants or explosives. Current fragmentation warheads using high explosive charges accelerate fragments to between 0.5 and 2.0 km/s. The muzzle velocity of some rifle bullets exceeds 0.9 km/s. A jet fighter can go 0.7 km/s full out and its air-to-air missiles may reach 1.2 km/s. One increasingly common and potentially confusing usage of "hypervelocity" describes the newest generation of advanced technology missiles which are pushing the envelope at 1.5 km/s. Long range ballistic missiles which leave the atmosphere at apogee reach 8.0 km/s but quickly decelerate to under 2.0 km/s due to drag during atmospheric re-entry. Therefore only speeds in excess of 2.0 km/s will be considered in the hypervelocity region.

One qualification to this definition is that only macroscopic and relatively massive particles (in this paper greater than 1.0 gram mass) are considered. Another consideration is that velocities of particles within the

atmosphere are bounded only by the limited amount of energy available in chemical reactions to overcome the atmospheric drag forces. In the near vacuum of space where drag is negligible, maximum velocities are only limited by the amount of available fuel. Finally, this working definition deviates from a commonly held one which states hypervelocities are those speeds "where the kinetic energy of the material is larger than its vaporization energy."[1] While this paper takes advantage of its implications, it is necessary to discard this condition at the lower end of the speed spectrum if all cases of interest are to be considered.

Since the ultimate speed limit of objects within the atmosphere is limited by the amount of energy available to push them against drag forces which increase with the square of velocity, it is necessary to develop means which impart energies greater than those currently realized by conventional chemical reactions if the 2.0 km/s speed barrier is to be broken. One of the best known and most researched methods to achieve hypervelocities is the Electromagnetic Railgun which uses a series a electromagnets to accelerate masses by converting electrical energy into a magnetic pulse which provides the motive force. The current state-of-the-art machine can accelerate a several gram projectile to speeds exceeding 8.5 km/s. Near term expectations envision a 20.0 km/s gun

while 100.0 km/s is the eventual goal. Railguns which were formerly one-shot devices have become reusable and in fact are acquiring a multi-shot capability which may culminate in a rate of fire of 60 rounds per second. While railguns look especially promising for space-based applications, they are severely restricted within the atmosphere because drag and aerothermal effects limit the stable flight of their long bullet like projectiles (a critical consideration for a single shot weapon) to less than 4.5 km/s. At these speeds, drag slows hypervelocity projectiles quickly making for extremely short effective ranges. Therefore, the railgun's effectiveness in the atmosphere is probably limited to close-in point defense situations such as those currently handled by the Navy's Phalanx CIWS.

One alternative hypervelocity method that may prove to be a viable component in a general endo-atmospheric intercept system is the Directed Energy Projectile Warhead (DEPW) which utilizes a specially configured high explosive warhead called an "imploding lens" to power a driving mechanism known as a shock tube which produces a narrow cone of hypervelocity fragments. Several advantages of this configuration are particularly noteworthy. First, in contrast to the railgun which fires one projectile at a time like a rifle, the DEPW acts like a shotgun covering an area described by the dispersion angle of the fragment

cloud, making it possible to relax the stringent accuracy requirements and still maintain an effective probability of kill. More important, however, is that while a railgun requires an extensive power supply and other support equipment, the DEPW is entirely self-contained and can even be fitted into a conventional intercept missile which provides the necessary mobility to compensate for the short effective ranges of hypervelocity particles within the atmosphere.

C. Study Approach

First a system concept was synthesized by examining the available literature on missiles, warheads, hypervelocity phenomena, coordinate systems, kinematics. lethality mechanisms and other pertinent topics. From this, mathematical models were developed and computer simulations programmed to evaluate system performance. Individual factors were then identified and analyzed to determine their contribution to overall performance. This process was evolutionary in nature; what began with a simple two-dimensional constant velocity zero drag scenario grew into a three dimensional model which simulates several different guidance schemes and is capable of evaluating hypervelocity warhead effectiveness while considering drag forces and complex relative motions.

D. Study Organization

This paper is composed of the main text which is divided into several sections, each of which deal with a specific aspect of the system. Mathematical equations and derivations have been moved to the appendices in the rear of the text when they do not contribute to the understanding of the text. Figures, graphs and tables are also grouped in the back of the paper.

II. DIRECTED ENERGY PROJECTILE WARHEAD

A. Configuration

The nominal configuration of the DEPW is shown in Figure 1. It consists of two basic components: an imploding lens warhead and an axial shock tube which fits inside the explosive charge. This basic design was initially developed by Gene McCall based on a proposal by Stirling Colgate for producing axial shock waves with phased cylindrical implosions.[1] Current research into this method is being conducted at the Los Alamos National Laboratory.

As discussed previously, chemical reactions have a limited energy availability (up to 5.0 MJ/kg) and detonation rate (maximum 8.8 km/s). Besides these innate limitations, energy conversion from the explosive blast to fragment kinetic energy is not 100% efficient. A conventional isotropic high explosive (HE) warhead transfers only about 30% of its explosive energy into kinetic energy while the DEPW may convert up to 90%; 50% energy conversion efficiencies are currently being achieved with shock tubes. Actual fragment velocities for conventional warheads are therefore limited to about 2.0 km/s and in most cases are significantly less. The DEPW gets around these limitations by using an intermediate working substance between the explosion and the

accelerating mass. As can be seen in Figure 1, a HE charge is wrapped around the cylindrical shock tube barrel at one end. At firing time, detonators initiate an explosion at the outer circumference of the charge. The shock wave created by the detonators and sustained by main charge initiation travels towards the center of the cylinder at a speed determined by the detonation rate of the explosives. The geometry of the warhead is designed so that the detonation wave reaches the entire length of the outer walls of the shock tube nearly instantaneously. By using a mix of fast and slow detonating explosives, the waves may be lensed more efficiently so that the detonation wave reaches the after end of the tube ever so slightly before the open end. This technique of phasing the arrival of the detonation waves is used to create the great velocities (up to 30 km/s) experienced by the working substance in the shock tube. Ordinarily a detonation wave encountering a hollow tube would simply crush or implode it. By putting low density CH foam (0.3 g/cm^2) in the center of the shock tube, the implosion is partially retarded and more importantly the vaporized foam becomes a working fluid which shoots out the free end of the tube at velocities greater than the phased detonation velocity and in effect creates the piston which accelerates the metal plate located further down the tube. Actual acceleration of the plate is achieved by the

gradual increase of hydrodynamic pressure as the working fluid expands to fill the intervening space. It is extremely important that the acceleration be gradual, continuous, and "shockless" to avoid vaporizing the metal plate or the macroscopic fragments that the plate is designed to form. An idea of the stresses in the accelerating plate can be gained by considering that the plate may go from 0.0 to 20.0 km/s in less than 0.7 microseconds, experiences a peak acceleration in the millions of g's and has a back pressure of over a million atmospheres. The current development of this method is still limited to laboratory situations with expectations for a system using 1.0 kg of HE to drive a 1.0 g mass to a speed of 20.0 km/s. Future weapons implementations should have a higher efficiency and will require a better charge to plate mass ratio. This study postulates using individual fragments massing between 1.0 and 25.0 grams making for a relatively heavy plate. On the other hand, the endoatmospheric applications considered in this paper make the higher initial firing velocities inefficient and only velocities between 2.0 and 12.0 km/s will be studied.

B. Hypervelocity Atmospheric Effects

All bodies moving through the atmosphere of the Earth are subject to drag forces which act to oppose the velocity of the object. The magnitude of the drag force

is commonly defined as:

$$F_{DRAG} = -\frac{1}{2} \rho_{\infty} V^2 C_D A_p \qquad (2)$$

where the free stream dynamic pressure, $\frac{1}{2} \rho_{\infty} V^2$, is a function of atmospheric density, ρ_{∞}, and the velocity, V, through the atmosphere. A_p is the projected area of the object, and C_D is the dimensionless coefficient of drag which is a function of the flow regime of the body. The flow regime for a body depends on altitude, mass, shape and size of the object. To simplify matters all bodies in this study are assumed to be perfectly spherical so that pellet size is directly related to the mass and density of the material. Further, for reasons to be examined, tungsten will be the only material considered. Thus for the fragment masses (1.0 - 25.0 grams) in the range of interest, pellet diameters vary between 4.6 and 13.5 mm. When this characteristic length is compared to the mean free path of air particles or the average distance between air particles at the altitudes of interest (less than 30.0 km), it becomes apparent that the pellet diameter is very much greater than the distance between the air particles (typically one ten millionth of a meter) which are tightly packed because of the relatively high atmospheric density near the Earth's surface. This means that the atmosphere through which the object passes can be modelled as a fluid

on a macroscopic scale since even an incremental movement of the pellet will impact so many air particles which rebound and hit other air particles that a classical fluidic boundary layer will be formed. Flows of this type are defined to be in the "continuum" flow regime. The continuum flow regime is further divided into compressible and incompressible regions. The Mach numbers, M, (the ratios of the bodies' velocity to the ambient speed of sound) dealt with in this work, which range from 6 to 40, greatly exceed the boundary value at M 0.5, placing our interest firmly in the compressible flow region. The coefficient of drag for this region is a function of the Reynolds number (a dimensionless quantity which relates the inertial forces of the body to the viscous forces of the fluid) and the Mach number. Specific calculation of the coefficient of drag for spheres in the compressible, continuum flow regime yields:

$$C_D = 0.92 - 0.38/M^2 \qquad (3)$$

where M is the Mach number.

Aerothermal effects comprise the other major consideration for endo-atmospheric hypervelocity pellets. At these extreme velocities great amounts of heat are generated and transferred to the projectile by impacts with air particles. This added heat increases the

pellet's temperature which in turn causes the pellet to radiate more heat. If the pellet's temperature rises to the melting point, the outer layer of material will begin to melt as more heat is added. This molten material will be quickly removed from the pellet by drag forces in a process known as ablation. Once ablation has begun the useful lifetime of the fragment becomes extremely short. This is because the mass loss decreases the kinetic energy of the pellet and hence its probability of kill as well as the pellet's radius, which in turn accelerates the ablation process. Since the pellet's utility decreases rapidly after ablation starts and because the equations describing the pellet become very complex and non-linear, this study limits the effective range of the projectiles to the range at which ablation begins. The calculation of this range may be considered in two parts. First, in order for ablation to occur the velocity of the particle must generate more heat than is being reradiated and the surface temperature must exceed the pellet material's melting point. If the pellet travels at a speed less than a certain critical velocity no ablation will occur and the range will not be limited. This critical velocity can be estimated by equating the aerodynamic heating rate to the reradiation rate at the melt temperature of the pellet which yields:

$$V_{CR} = \left(\frac{8 \epsilon \sigma T_m^4}{\eta \rho_\infty} \right)^{1/3} \qquad (4)$$

where ϵ is the surface emissivity (.36 for tungsten), σ is the Stefan-Boltzman constant (5.67×10^{-8} W/m^2K^4), T_m is the melting temperature (3650 K for tungsten), η is the aerothermal heat coefficient (a non-dimensional constant less than 0.05 for the considered altitudes and masses), and ρ_∞ is the atmospheric density. Since critical velocity is most strongly a function of melting temperature, tungsten is a natural choice for the material composition of the fragments because of its extremely high melting point and the added advantage of high density (19,600 kg/m^3) which allows greater kinetic energy per unit volume. When drag effects are taken into account there is another critical velocity to be considered. It is conceivable that a particle travelling initially faster than the critical velocity will be slowed by drag to below the critical velocity before the ablation point is reached. This upper limit is given by:

$$V_{CR/DRAG} = \left(\frac{2 C_D H_m}{\eta} \right)^{1/2} \qquad (5)$$

where C_D is the coefficient of drag, H_m is the latent heat of the material at the melting temperature (570 kJ/kg for tungsten), and η is the aerothermal heating coefficient. Finally, the equation which solves for the time of flight

to melt, t_m, which can be substituted back into the drag equations to determine the maximum effective range if required, is:

$$t_m = \frac{S_o}{V_o}\left[\left(1 - \frac{2C_o H_m}{V_o^2 \eta}\right)^{-1/3} - 1\right] \qquad (6)$$

where V_o is the initial velocity, and S_o is a drag constant derived in appendix A. One study sponsored by Los Alamos National Laboratory puts the first critical velocity for the pellets of interest at around 1.7 to 3.0 km/s while the second set of critical velocities which consider drag have "worst case" lower bounds of 5.0 to 7.0 km/s.[2] Even above these critical speeds, by limiting this study to velocities less than 12.0 km/s and effective ranges of less than 200 m, ablation effects can be ignored.

While this analysis includes the major endo-atmospheric interactions including drag, aerothermal heating, radiation cooling, and ablation by melting, it is by no means all inclusive. Many other phenomena act on hypervelocity pellets within the atmosphere but their contributions are either minimal or are not well understood requiring further experimentation to characterize them. Some of these effects include chemical reactions between the pellet and air molecules, heat conduction within the pellet, sputtering, melt layer

interactions, and vaporization effects.

C. Lethality

The final effectiveness criterion for any warhead is its lethality or ability to neutralize a target. All warheads rely on transferring stored energy, whether kinetic from inherent motion or chemical from an explosive charge, to the target to disrupt its proper operation. Typically this energy is transferred by blast or shock wave or by high speed fragments. A conventional isotropic fragmentation warhead expends its energy equally in all spatial directions, as evident in Figure 2, with about 30% of the energy going to accelerate its fragments while the remaining 70% contributes to the blast effects. Blast waves represent the rapidly expanding region of high pressure gases that are formed by the detonation of high explosives. The strength of the blast effects attenuate as the volume of the gas increases making it inversely proportional to the cube of the distance from the center of the explosion ($1/R^3$). The expanding gases also shatter the explosive's casing and accelerate its fragments. The density of these fragments, depending on warhead design, attenuates at a rate between the reciprocal of the square of the distance to the blast ($1/R^2$) and simply inversely proportional to the distance from the blast ($1/R$). The DEPW on the other hand is a highly directional warhead

which utilizes almost all of its energy (90%) to accelerate its fragmentary mass. Attenuation rates are still inversely proportional to the square of the distance travelled ($1/R^2$) but the warhead gain, a measure of relative effectiveness, is dramatically boosted (see Table 1) by a factor of:

$$\text{DEPW GAIN} = \frac{16}{\Theta_0^2} \qquad (7)$$

where Θ_0 is the dispersion angle (in radians) of the cone of expelled projectiles. Gain increases as the dispersion angle decreases and when it reaches zero the gain becomes infinite and the projectiles fly in parallel trajectories never dispersing. As an example a DEPW with a 5 degree dispersion angle is about 2500 times more effective than an isotropic warhead at the same range given the same number of equally sized fragments travelling at the same speed. Of course all of these values will not be identical. Fragment velocity, for instance, is primarily a function of the explosive's power and the charge to mass ratio for a conventional warhead while the DEPW's velocity depends solely on the design of the imploding lens charge. As discussed previously the velocities produced by the DEPW may be an entire magnitude above those of conventional warheads. This makes DEPWs less sensitive to engagement geometry requirements unlike some warheads

which require a head on encounter to take advantage of the target's velocity contribution to the total impact speed. When translated in terms of kinetic energy this means a potential lethality gain of 100 times the current effectiveness. The critical parameters for the DEPW will be the total mass of the warhead and the required charge to mass ratio. Current intercept missiles carry warheads ranging from 20.0 to 80.0 kg. This means that with the current estimated charge to mass ratio of 1000 only about 75.0 grams of fragments will be able to be accelerated by the DEPW. In contrast the charge to mass ratio for a conventional fragmentation warhead is on the order of 0.5 giving it a lethality gain of 2000 over the DEPW. Even at this mass disadvantage the DEPW shows a lethality gain of several magnitudes over the isotropic warhead if the DEPW's guidance system is accurate enough to place the target within the dispersion angle of the warhead. This quick analysis is by no means rigorous and is only intended to examine the DEPW's potential effectiveness. Detailed analysis will have to wait until an actual warhead is constructed and tested.

The specific fragment lethality mechanisms are very important in evaluating the effectiveness of a warhead. While kinetic energy has already been linked to destructive potential it is by no means the only factor. Momentum, which is the mass of the fragment multiplied by

the impact velocity, plays a significant role where plastic deformation from impact can warp target components, seriously degrading their operation. Energy density, the energy delivered per unit area of the impact surface of the target, contributes to the overall structural kill capability. Kinetic energy, of course, plays a key role. The volume of target material displaced, which is given by the depth of penetration multiplied by the cross-sectional area of the hole, by an impacting fragment has been shown to be directly proportional to the terminal kinetic energy of the fragment. While these relationships have been experimentally validated for high speed particles, they may not completely characterize hypervelocity impacts where the kinetic energy of the fragment greatly exceeds the vaporization energy of the materials involved, which means that the fragment will act as a fluid rather than a solid during the time of impact. That is not to say that hypervelocity impacts are less effective, in fact, the opposite is more likely to be true. Initial testing of hypervelocity lethality has shown that a 2.5 gram plastic cube travelling at 8.6 km/s can easily penetrate a 6.5 mm steel plate. More experimentation is needed to gain a better understanding of hypervelocity lethality mechanisms. The velocities required to melt (1.23 km/s) and vaporize (3.35 km/s) tungsten on impact put the

velocities of this study right on the "hypervelocity" threshold. In addition to the effects already discussed there are certain synergistic effects where the damage caused by two or more fragments striking a target nearly simultaneously causes damage that is greater than the sum of the individual contributions if the fragments hit the target singly. This phenomenon occurs when two or more fragments impact the target area very close together during a short period of time, nominally 10 microseconds, so that their shock waves are superimposed on each other. While the general lethality mechanisms can be identified and most are well understood, it is impossible to discuss specific kill criteria without detailed consideration of specific targets. Since there is so much variation in the configuration, construction, and capabilities of potential targets this approach is unrealistic except when considering highly specialized systems with well defined parameters. On the other hand a general figure of merit (FOM) based on general structural kill capabilities is feasible and desirable. One formulation which has been advanced in the literature[3] is the geometric mean of energy and energy density which is given by:

$$FOM = \frac{N\, m\, V^{\lambda}}{\lambda \sqrt{A}} \qquad (8)$$

where N is the number of fragments impacting (which should

be greater than 50), m_{FRAG} is the mass of each fragment, V is the impact velocity, and A_T is the cross-sectional impact area of the target. Dimensional analysis of this formula shows that the FOM is given in newtons. A reasonable minimum effective value to kill most targets is 1.0 million newtons.

D. Warhead Model

In discussing the fragment-target interaction model given in Figure 3, several parameters and assumptions must be defined. All fragments are assumed to be spherical and of equivalent mass and size. All assumptions used in determining drag and ablation effects apply. Θ_D is the dispersion angle measured as the full plane angle from one boundary of the fragment cone to the other and also bounds the three standard deviation (3σ) limits of the normal circular pellet distribution. Bore diameter, D_B, is exactly what it claims to be. Target cross-sectional area, A_T, is assumed to be constant and independent of orientation. V_{FIRE} is the mean velocity of the pellet fragments as they leave the bore. The velocity distribution of fragments is assumed to be normal or gaussian and be bounded by the three standard deviation value (3σ) given as a percent of V_{FIRE}. V_{FRAG} is the time varying inertial velocity of the fragments which accounts for the missile's velocity component along the

firing axis, drag effects, and velocity deviation. R_I is the range from the position of warhead detonation to target impact. V_{TR} is the relative velocity of the target with respect to the point of warhead detonation and consists of the target velocity, V_T, the normal components of the missile velocity, V_M, with respect to the firing axis, as well as the missile rotation rates at detonation time. In modelling this system, the center of gravity of the missile is frozen in position at warhead detonation and becomes the origin of a special coordinate frame which is oriented along the firing axis of the warhead which is assumed to be coincident with the existing missile body (B) frame. The target is then moved with respect to the firing point using V_{TR} to advance its position at regular time intervals. When the target comes inside the projected fragment cone the time from firing is used with V_{FRAG} to determine if a hit is possible. If a hit is possible the lethality figure of merit is computed for that time interval by evaluating the volume of space the target traverses for pellet density and energy delivered. This incremental process continues until the target has moved outside the projected fragment cone. By using this unorthodox reference frame the major components of the fragment's initial velocity can be grouped together so that the highly non-linear drag effects detailed in Appendix A can be evaluated accurately. This arrangement,

by consolidating all other velocities, also precludes having to translate or rotate the fragment cone because the relative velocities are conserved. This model does, however, assume that the missile's velocity is nearly coincident with the missile heading (good for angles of attack less than about 15 degrees using the small angle approximation).

III. INTERCEPT MISSILE

A. Missile Configuration

Almost all intercept missiles share the same types of components. A rocket engine or very rarely a jet engine is used to expel hot gases from an exhaust nozzle fitted to the rear of the missile to provide the means of motive force. Some form of sensor, usually either radar or infra-red, is used so that the missile can "see" its target. This information is then passed to the guidance computer and missile autopilot which generate lateral acceleration commands to correct course and insure an intercept trajectory. The missile may also have the capability to receive target information and/or guidance commands by radio data link so that it may maneuver to intercept even if its own sensors can not "see" the target. Steering the missile is accomplished in one of three ways, each of which has its own advantages and disadvantages. Aerodynamic control surfaces such as fins, wings, and canards, are turned by servo-motors responding to acceleration commands. Each aerodynamic surface produces a lift force proportional to its angle of deflection which causes a lateral acceleration changing the path of the missile's movement and a torque which changes the missile's heading. Aerodynamic control's major drawback is that the amount of lift force produced

varies greatly from situation to situation because of non-linear aerodynamic effects. Alternatively the exhaust nozzle of the missile can be tilted to produce off axis thrust components which also produce lateral acceleration and turning torque. This method, called Thrust Vector Control (TVC), while capable of providing large turning forces, is clearly only effective while the rocket still has fuel to burn. Finally there is the Reaction Control System (RCS) which uses small precision rocket thrusters built into the missile perpendicularly, which fire on command in a certain sequence to accurately produce the desired lateral acceleration and turning rate. Its main limitation is also the limited amount of fuel available for acceleration. This paper is not particularly concerned with which method is used so long as the lateral acceleration and turning requirements needed to intercept the target can be satisfied. The final and most important component, at least as far as this study is concerned, is the warhead, which must be mounted axially in one of two configurations, as shown in Figure 4. While this study only examines the forward firing case, the reverse configuration should not be ignored. Although some intercept missiles rely on hitting the target directly, most missiles rely on their warheads to transfer the requisite destructive energy to the target. In intercept systems which do rely on warheads, the overall

effectiveness of the system relies heavily on the ability of the fuze to calculate and then detonate the warhead at the precise instant of maximum probability of kill.

A better understanding of exactly what this DEPW delivery system entails can be gained by examining some of the general characteristics of existing intercept missiles. A surface or air launched medium to long range intercept capability should be the goal. This puts it in the class of the U.S. Army's Patriot surface-to-air missile, the U.S. Navy's Standard 2 ship-to-air missile and the U.S. Navy's Phoenix air-to-air missile. All of these missiles are 0.35 to 0.4 meters in diameter, are 4.0 to 5.0 meters long, and weigh between 500.0 and 1000.0 kg. Mass of the warheads lies in the previously stated range between 40.0 and 80.0 kg. Maximum speed and range for the surface launched missiles is about 1.0 km/s and 50.0 km. The air launched missile however can travel nearly 1.5 km/s and can reach 150.0 km.

B. Simplifying Assumptions

In order to evaluate the intercept system's overall effectiveness it is necessary to evaluate the performance of the warhead's delivery vehicle, especially its maneuverability and stability, which affect the pointing accuracy of the warhead. Two major problems become

readily apparent in modelling missile performance and its contribution to system effectiveness. First the overall complexity and the sheer number of factors which have been identified to characterize missile performance makes simulation a herculean task. It also becomes extremely difficult to identify and analyze the critical factors which determine the performance parameters of interest. A simple solution to this problem is to streamline the equations describing missile performance by making simplifying assumptions and by limiting the number of independent variables. The second problem occurs because good estimates of some parameter values are not available due to classification or because they will simply not be known until an actual missile is designed, built and tested. This problem can be minimized in the same way through simplification of the model. Those critical values that remain unknown can then be removed by reformulating the equations or be replaced with normalized (non-dimensional) parameters which can be varied through a range of possible values.

The first simplifying assumptions deal with the environment in which the missile operates, namely the Earth and its surrounding atmosphere. The Earth in this study is assumed to be a flat, fixed and non-rotating inertial frame. This scheme facilitates the use of a rectangular coordinate system, avoids the need for

spherical geometry and allows us to ignore Coriolis acceleration for bodies travelling in circular paths (which is at most 1/10 of a g (.98 m/s^2) for objects travelling at orbital velocities). The second set of assumptions allows us to ignore the effects of the Earth's relative motion through space and its rotation about its axis which are negligible in any case. Further it is assumed that the atmosphere is completely static --i.e. no wind-- and that the Earth's gravitation, equivalent to 1.0 g (9.8 m/s^2) at the surface but which decreases with altitude, is insignificant in comparison to the many g's acceleration experienced by the missile in maneuvering to hit the target. The target is assumed to be a point mass which moves at constant velocity.

The missile itself is assumed to be a rigid body. This approximation ignores the bending and twisting of the missile body which occurs when forces and torques are applied in maneuvering so that the equations of motion do not have to account for these highly non-linear effects. Symmetry around the long axis of the missile (a circular cross-section) is also assumed which simplifies the moment equations. Another obvious assumption which simplifies the moment equations is that the length of the missile is very much greater than the diameter. Mass and mass distribution of the missile are assumed to be constant. Real missiles lose mass as their rocket motors burn and

hot gases are expelled from the nozzle. This effect which is ignored tends to move the center of gravity of the missile forward changing the static stability margin of the missile which partially determines its maneuverabilty.

Initial studies assume that the missile's velocity vector is coincident with the missile's heading, making for a constant angle of attack equal to zero. Later developments allow for a more realistic handling of angle of attack and will be discussed in a later section. Drag forces are neglected and instead an arbitrary maximum equilibrium speed is used to correlate when the thrust force from the rocket equals the retarding drag force. Acceleration of the missile is assumed to be constant until the drag equilibrium speed is reached. Along with drag, lift and side forces are ignored in the initial study.

Mathematical models of missile motion derived from these assumptions are presented in Appendix B.

C. Coordinate Systems

In examining a system's performance, a method of quantifying the positions, velocities, and accelerations for both the missile and the target in terms of magnitude and direction is required. This is accomplished by superimposing a rectangular coordinate system with three perpendicular metric axes over the three dimensional space

of interest. All quantities of interest are then measured from the origin with respect to its axes. Three distinct coordinate systems, as seen in Figure 5, are used in this study. The first is the Earth based or inertial (I) frame which has its origin at an arbitrary point on the Earth's surface and its positive axes aligned in the North, East, and Down directions respectively. This arrangement requires altitudes above the surface of the Earth to be negative in sign, an unexpected result, which is required to conserve the right-handed coordinate system so that all equations are consistent in determining the sense of positive and negative directions. From this frame of reference the trajectories of both the missile and the target are seen as they truly move through space. The next is the missile vertical (V) frame with its origin at the center of gravity of the missile and its axes aligned with the inertial (I) frame in the North, East, and Down directions. This frame serves as an intermediate step in converting coordinates from the inertial (I) frame to the missile body (B) frame and vice versa. The final reference frame shown in Figure 6 is the missile body (B) frame which is also centered on the missile's center of gravity but which has its axes oriented with the missile body so that it provides a perspective as if someone was riding inside the missile's cockpit and looking out. The primary axis which points forward along the length of the

missile body is labelled the x axis and sometimes called the roll axis. The other two axes are somewhat arbitrary for missiles because of their inherent symmetry. The y or pitch axis is at a right angle to the x axis and would point out of the right wing of a normal aircraft. Similarly, the z or yaw axis is perpendicular to the other two axes and points out of the underside of the aircraft towards the ground when in level flight.

Obviously, the view for an observer in the inertial (I) frame differs greatly from the perspective of an observer in the missile frame when they look at the same thing. Vector analysis can be used to translate the observed values from one point to another such as from the I to V frames and back again. The missile orientation, however, will rarely be aligned with the inertial axes making it necessary to transform the observed coordinates into the new coordinate system by rotating the axes as between the V and B frames. Three basic methods are used to describe the relative orientation between coordinate frames as well as transform between them and calculate the required rotational rates needed to treat an object's motion in three dimensions. The most common method utilizes Euler angles which defines the orientation of the new coordinate system in relation to the original coordinate system with three angles (ϕ , Θ , Ψ) which represent the angular deflection between the old and new

x,y,z axes through a rotation around the old y,z,x axes respectively as detailed in Figure 7. While this method provides a good idea of the physical orientation of the system, it has major shortcomings because the equations used to transform coordinates and determine the angle's time derivatives (rotational rates) are trigonometric and are subject to singularities. The second method relies on the direction cosines between the axes to generate a 3x3 Direction Cosine Matrix (DCM) which is used to transform vectors from one frame to another. The only drawback to this system is that it contains six redundant parameters which makes it inefficient for other calculations. The last method, which has been mainly ignored until recently, uses quaternions, which are a set of four artificially derived parameters that describe orientation in three dimensions. While these parameters have no analogous physical representation in the systems they describe, they are particularly efficient in calculating orientations and time rates of angular change (Appendix C).

D. Aerodynamic Transfer Function

While the initial study ignored aerodynamic effects for the sake of simplicity, missile dynamic response to acceleration commands plays a critical role in aiming the warhead. Previously, it was assumed that the missile responded instantaneously to guidance commands, but as

with any real system this is physically impossible due to inherent time lags. The actual response of the system, in this case its actual lateral acceleration, can be described with an aerodynamic transfer function. It has been shown that the missile rotation response can be adequately modelled with a second order system. One other time lag that must be considered is the incidence lag which describes the condition where the missile's velocity vector lags the direction of the missile's current heading, an angle which is described as the angle of attack. Referring to Figure 8, the input, which is the commanded lateral acceleration, produces missile body rotation rates which are used in the translational and rotational kinematic equations. Missile velocity rotation rates are then calculated by applying the first order incidence lag. Actual lateral acceleration can be found by multiplying the velocity rotation rate by the forward translational velocity. The terms ω_n and ζ represent the natural frequency and damping coefficient of the missile's phugoid or short period mode which characterizes its turning response. τ is the first order incidence time lag which gives the angle of attack required per unit turn. All of these values are a function of specific missile design, the coefficients of lift, missile velocity, and altitude. It should also be noted that this model assumes linear aerodynamics which offer good approximations of

actual performance for angles of attack not exceeding 20 to 40 degrees.

IV. GUIDANCE SYSTEM

A. Boost and Midcourse Phases

Missile flight has three phases as detailed in Figure 9. In the initial or boost phase, the missile accelerates at maximum thrust to clear the launcher and reach its nominal flight speed. During the second or mid-course phase, the missile travels toward the general area where intercept will occur by either coasting or using a less powerful sustainer rocket motor to keep its speed up. During the terminal phase, the missile uses available sensor information to maneuver to hit the target or put it in the most favorable geomtery for the warhead to do so.

The boost phase begins at launch. Most surface launched missiles are on rail launchers that are aligned with the target or the projected intercept point before the missile fires its booster. A new method which is becoming more common is the vertical launch technique where the missile flies straight up and after clearing the launcher performs a pitchover maneuver to better align itself with the intended intercept point. Air launched missiles which are already travelling at the speed of the launching aircraft, initially fly out in the direction they were mounted on the aircraft. Guidance commands during the boost phase are therefore simple. Basically all lateral acceleration is held to zero until the missile

safely clears the launcher and the boost motor runs out of fuel or a minimum stable flight speed is reached, except in the case of an initial pitchover maneuver where the stored lateral acceleration commands, which are calculated by the firing platform before launch, turn the missile towards the target while the missile is still travelling relatively slow.

Midcourse guidance is designed to keep the missile heading towards the target until the missile's own sensors can acquire and lock onto the target. If the missile's sensors are powerful and accurate enough to find the target right after boost this phase may be skipped completely. There are two common methods for midcourse guidance. The first and simplest is for the missile's autopilot to maintain the course and speed at which it was launched and hope that it finds the target. A more effective variation of this system is for the missile to fly an intercept trajectory calculated by the launch platform before boost. Clearly this technique has major shortcomings especially considering today's highly agile targets which make predicting future target position impossible beyond a very short time interval. The second, more complex and effective system is called command guidance. This system uses the more powerful sensors and computing facilities of the launch platform to track the missile and target and to generate new lateral accleration

commands for the missile which are then transmitted by radio data link. Alternatively, only tracking information from the launch platform's sensors may be transmitted to the missile which calculates the necessary intercept command accelerations internally. The main limiting factor for this type of system is that there is an inherent time delay because of the time it takes light to travel from the target and missile to the platform's sensors, the time used to process this information into usable form, the time required for the computer to generate the guidance commands, and finally the time it takes the radio signal to reach the missile. During this interval neither the target nor the missile will have remained stationary, making the guidance commands, which were calculated with their former speeds and positions, out of date. While the inaccuracy due to time lag involved with this method makes it impractical during the terminal missile phase, which requires quick reaction times to be responsive to target maneuver, it is accurate enough to be used during the midcourse phase when the missile and target are still at some distance from each other.

B. Terminal Homing Guidance

As discussed previously, the terminal phase of a missile's flight is characterized by the need for quick

reaction time and high maneuverabilty to make last minute flight corrections in response to target maneuver as the time to closest point of approach decreases rapidly. The primary way to decrease reaction time is to make the missile entirely self contained so that the communication times between the different components are minimized. This means that the missile must carry its own sensors and guidance computer. Sensor capability, however, which is primarily determined by sensitivity and range, is limited by the size and mass of the components that can be fitted into a missile.. Therefore, the terminal phase of the missile can be considered to begin when the target gets in range of and is acquired by the missile's own sensors. This type of guidance, which relies solely on internal components, is known as "homing" guidance. Information collected by the sensors is passed to the guidance computer where a guidance law processes it and produces a lateral acceleration command which causes the missile's control components to alter the missile's course.

All homing guidance laws considered in this paper can be derived from the general guidance equation, determined from the geometry given in Figure 11, as:

$$\gamma_c = K\Theta + \phi \qquad (9)$$

where γ_c is the desired missile flight path angle relative

to an inertial reference, Θ is the line of sight (LOS) angle between target position and the reference, K is the guidance gain, and ϕ is a constant lead angle. Four guidance laws, pursuit, lead angle, predictive, and proportional navigation, are considered in some detail and one other technique, optimal control, is mentioned in passing.

1. Pursuit Navigation

Pursuit navigation is the simplest type conceptually and mathematically. A missile using pursuit navigation will always fly so that its velocity vector points directly at the instantaneous position of the target (Figure 12). This means that for a moving target the missile will eventually end up in a tail chase configuration except if the target and missile always fly exactly towards each other, in which case they will hit head on. Mathematically, this corresponds to a guidance gain, K, of unity and a zero lead angle ($\phi = 0.0$) so that the equation becomes:

$$\gamma_c = \Theta \qquad (10)$$

Performance for this type of system has several unfortunate constraints. The first, because of its "tail chase" nature, requires that the speed of the interceptor must be greater than the speed of the target in order to

close the range. The second constraint limits the missile's top speed to twice that of the target's because required lateral acceleration demands can be shown to go to infinity beyond this point. A corollary to this constraint also shows that only missiles initially in the rear hemisphere of the target's flight path may engage it without requiring infinite lateral accelerations. It should be kept in mind that these constraints are formulated on the assumption of constant target velocity, constant missile speed, and that the missile will achieve a direct hit. Actual missiles, with lateral acceleration limits somewhat less than even the finite acceleration requirements for missiles travelling less than twice as fast as the target, may not be able to achieve direct hits for many engagements. It may, however, still be possible for the missile to get close enough to the target for the warhead to be effective; this is particularly true for missiles approaching from ahead of the target.

One way of implementing pursuit guidance in an actual missile is to use the measured angle between the missile heading (assuming it is coincident with the velocity vector) and the target's position in the missile body (B) frame. This angle, Θ_M, is then used to generate a lateral acceleration command:

$$n_c = \frac{V_m \Theta_m}{t} \qquad (11)$$

where n_c is the magnitude of commanded lateral acceleration, Θ_m is the target line of sight angle from the missile, V_M is the missile's speed, and t represents the time between sensor measurements. The direction in which the acceleration is to be applied is easily calculated from the target's coordinates in the B frame so that the normal acceleration vector points to the target's position as it is projected on y-z plane of the B frame.

2. Lead Angle Navigation

Lead angle navigation is very similar to pursuit navigation except that a constant lead angle, ϕ, is included:

$$\gamma_c = \Theta + \phi \qquad (12)$$

This causes the missile to keep the target at an angle, equal to the given lead angle, with respect to the missile's velocity vector throughout the entire flight (Figure 13). Regardless of the missile's initial position, the final approach to the target will be along a specific angle just as all engagements with pursuit navigation (which is effectively a zero lead angle) approach the rear of the target. This approach angle is given by:

$$\text{APPROACH ANGLE} = \text{ARCSIN}\left[\frac{V_M}{V_T} \sin \phi\right] \qquad (13)$$

where V_M is the missile speed, V_T is the target speed, ϕ is the lead angle. Clearly if the product of the sine of the lead angle and relative velocity exceeds unity the arcsine will become undefined and intercept will be impossible. Lead angle intercepts also suffer from the same constraints that pursuit cases do. However, the upper missile velocity limit to avoid unbounded lateral accelerations is a function of the lead angle:

$$\frac{V_m}{V_T} \geq \frac{2}{\sqrt{4 - 3\cos^2\phi}} \qquad (14)$$

Implementing this method is also similar to the pursuit case except the absolute value of the difference between the targets LOS angle, θ_m, and the lead angle, ϕ, is used:

$$n_c = V_m(\theta_m - \phi) \qquad (15)$$

3. Predictive Navigation

This navigation scheme is variously known as predictive, constant bearing, or collision course navigation. It is intuitively clear that the shortest path between two points is a straight line and that a missile travelling along the shortest distance to a point

at a constant speed will take the least amount of time. Predictive navigation then predicts the trajectory of the target using current information and then determines the interception point with known missile perfomance and finally calculates the straight line trajectory to the interception point from the missile's current position and generates the appropriate commands to turn the missile to the collision course (Figure 14). There is, however, a much easier formulation by realizing that a straight line collision course will occur if the missile can match the target's velocity in the direction perpendicular to the LOS between the target and missile assuming that the range along the LOS is decreasing. This leads to the following equation:

$$V_M \sin \Theta_M = V_T \sin \Theta_T \qquad (16)$$

where V_M is missile speed, V_T is target speed, Θ_M is the LOS angle with respect to the missile velocity vector, Θ_T is the LOS angle with respect to the target velocity vector. By rearranging the equation and substituting ϕ for Θ_M, the required lead angle to maintain a collision course may be calculated to be:

$$\phi_c = \frac{V_m}{V_T} \sin \Theta_T \qquad (17)$$

This value can easily be substituted into the equations derived for lead angle intercept without difficulty to determine magnitude of acceleration. Direction of acceleration is in the interception fly plane as described in the proportional navigation section. The only remaining problem is finding the values of θ_T and V_T using only information that is readily available to the missile through sensors. This can be accomplished by using the equation for relative tangential velocity of the target with respect to the missile and the LOS:

$$R\dot{\theta} = \pm V_M \sin\theta_M \pm V_T \sin\theta_T \qquad (18)$$

where R is the range or distance between the missile and target and $\dot{\theta}$ is the angular rate of change of the LOS. Since R, V_M, θ_M, and $\dot{\theta}$ can be measured by sensors the term, $V_T \sin\theta_T$, can be found by solving for it where the signs are determined by the relative geometry of a particular case.

Predictive navigation is very attractive for several reasons. It minimizes interception time and maximizes the range of the engagement envelope by flying a straightline interception course. It is also very effective against maneuvering targets as it has been shown that if missile and target speeds are constant, the required lateral acceleration of the missile will always be less than that

experienced by the target. Its one major constraint is that it requires more information and thus more capable sensors and computers than any other homing guidance method. Care must also be taken to limit the gain of the acceleration command or it will quickly become unstable.

4. Proportional Navigation

The most commonly used method of homing guidance is proportional navigation which is relatively easy to implement and produces excellent results. The mathematical description of this concept is simply the first time derivative of the general guidance equation which yields:

$$\dot{\gamma} = K\dot{\theta} \qquad (19)$$

where $\dot{\gamma}$ is the required turning rate of the missile, K is the effective navigation ratio (guidance gain), and $\dot{\theta}$ is the time rate of change of the LOS with respect to the missile. Missile trajectory is characterized by large initial lateral accelerations which decrease steadily as the missile gradually comes to a constant bearing (straight line collision) course (figure 15). The effective navigation ratio, K, is composed of several terms:

$$K = N\left(\frac{V_R}{V_m}\right)\frac{1}{\cos\phi} \qquad (20)$$

where N is the true navigation ratio, V_R is the magnitude of the relative closing velocity, V_M is the missile speed, and ϕ is the required lead angle. The true navigation ratio, N, is usually a number around 4 which provides adequate response time while maintaining stability. Navigation ratios of less than 2 cause a demand for infinite lateral acceleration as the target is approached. A navigation ratio of 3 has been shown to be the most efficient in terms of total acceleration demands. While ratios greater than 5 offer faster response times, they cause extremely high initial acceleration demands and tend to be less stable. The velocity terms are included to account for differing relative geometries. The geometric gain, $\frac{1}{\cos\phi}$, also compensates for the relative geometry but is usually ignored or set to a constant ($\sim .85$) because of the difficulty in computing the lead angle.

It is then a simple matter to implement this guidance law using the time rate of change of the LOS angle with respect to missile heading, $\dot{\theta}_m$:

$$n_c = K V_m \dot{\theta}_m \qquad (21)$$

Determining the direction of the lateral acceleration in three dimensional space, however, is somewhat more difficult. First the interception plane which is the two

dimensional plane describing the target's relative motion with respect to the missile's current position is found by taking the vector cross product of the target's relative position vector with the target's relative velocity vector. The acceleration vector lies within this plane and is by definition perpendicular to the missile's velocity vector so that it may be found by taking the cross product of the missile's velocity vector and the intercept plane's description vector.

5. Optimal Control

Optimal control techniques which have been developed in the field of control systems engineering are useful in solving specific performance problems. These methods have been used, for example, to maximize the range of missiles by optimizing their flight paths by commanding them to take a more ballistic trajectory to allow gravity to assist their flight as well as take the missile higher where the air is thinner and the retarding effects of drag are lessened. These techniques can also be used to show that the proportional navigation scheme with a navigation ratio of 3 is optimum in minimizing the total lateral acceleration requirements. While beyond the scope of the current work, these techniques should be examined to determine the effectiveness of optimizing several of the parameters of the DEPW and associated systems.

C. Sensors

The actual mechanisms which provide the necessary guidance information rely on detecting and interpreting the various forms of electromagnetic energy that are generated or reflected from the target throughout the spectrum ranging from the micro- and milli-meter waves through the conventional radio and radar frequencies to the visual and thermal wavelengths at the opposite end. Actual external sensors may be of several types. Passive sensors only receive energy emanations and can only give angular bearing information including angular rates of change. Active systems transmit energy towards the target and rely on the reflected returns to produce usable information. Active systems can provide range and range rate (by virtue of the Doppler Effect) information in addition to angular and angular rate information. Semi-active systems also rely on reflected energy from the target but in this case the target is illuminated by a third source. Angular and angular rate information are commonly supplied while in some complex systems range can be deduced. External sensors are either body-fixed or gimballed and are generally physically constrained to look-angles, LOS bearing angles, of less than 45 degrees from missile heading. Body-fixed sensors as the name implies are attached directly to the body and cannot move. Gimballed sensors are gyroscopically stabilized and

decoupled from the motion and rotation of the missile allowing sensors to be aimed at the target, making for a smaller field of view requirement and better sensitivity. The term sensors also includes internal instruments such as accelerometers, gyros, and altimeters which provide information on the missile's own state. Performance of all of these sensors can be increased dramatically by using information processing techniques to produce more accurate values for the measured quantities and in some cases even deduce values of parameters that are not directly measured but which are necessary for calculations.

Although this study is not concerned with choosing or designing a sensor system, except to insure that the proper information is available for the guidance law, due consideration should be made of several points. The overall cost effectiveness of the weapon system, which will be the final production criterion, is strongly dependent on the complexity of the sensor suite. The more accuracy and the greater amount of information that is required, the more complex and more expensive the sensor will become. Also internal sensors, passive sensors, and fixed-body sensors tend to be less expensive than their counterparts; they do, however, tend to require more information processing to achieve the same level of performance. This may be a critical point since the cost

of sensors has been steadily increasing while the cost of microprocessors steadily decreases even as their speed and capacity increase. It may therefore be more cost effective in the long run to concentrate on information processing intensive systems over sensor intensive ones.

V. RESULTS AND DISCUSSION

The major quantifiable result of this project was the development of an effective computer simulation code using ACSL (Advanced Continuous Simulation Language) and FORTRAN. Modelling the complex dynamics of missile flight and hypervelocity lethality was an evolutionary process. The first and simplest models were specialized two dimensional, constant velocity simulations that validated certain aspects of theory and contributed to the overall understanding of the system concept. By gradually removing simplifying assumptions, the conceptual model and computer simulations became more complex until it was necessary to reformulate the algorithms and consolidate the various simulations of the individual components into one program titled MISDYN which is listed in Appendix D. This program is a fully three dimensional simulation of the terminal homing phase from target acquisition to warhead detonation and then through pellet flight to final lethality evaluation at impact.

The terminal homing phase of simulation models missile flight which can be governed by any of the four guidance laws described in section IV. Graphs 1 and 2 display some of the characteristics of a typical proportional navigation trajectory. Graph 1 shows the missile line of sight angle, Θ_M, and the lateral acceleration, n_c,

requirements. As expected theta converges to a constant lead angle as it approaches the target. Lateral acceleration (ac) also decreases as the straightline collision course is achieved. Several other noticeable modelling phenomena are evident on curve B. No lateral acceleration exists during the first half second of flight which corresponds to the boost phase. Also the maximum acceleration limit of the missile is evident when acceleration levels out abruptly for several seconds. Graph 2 shows the relative position and velocity of the target in the missile body coordinate system.

The other major component of the simulation evaluates lethality figure of merit by determining the number and kinetic energy of pellets that will impact the target. Table 3 shows several computed values assuming a nominal 75.0 gram plate mass as range and initial velocity are varied. It is apparent that these values fall short of the 1.0 MN of force required for target destruction. The right most column gives the gain required in each case to meet this minimum requirement. Gain can be raised by increasing any of the parameters detailed in equation (8) or by narrowing the dispersion characteristics of the fragment cloud by adjusting the standard deviations of pellet density which are functions of range, dispersion angle and percent velocity deviation.

As previously determined, overall effectiveness of the

DEPW relies on the pointing capability of the missile to align its firing axis with the target's future intercept position which depends very strongly on initial intercept geometry and relative motion. An idea of the required pointing accuracy can be acquired by assuming that axial dispersion of the fragments is zero so that the pellets propogate as a two dimensional disk. The percent of pellets that actually impact the target can then be found by using Graph 3, where the total number of fragments impacting relies on the aim bias or lateral miss distance which is simply the distance between the centroid of the target and the firing axis in the plane where the fragment disk intersects the target area (see Figure 16). It is also a function of target area which is assumed to be constant and circular in nature, and of the angular standard deviation, σ, which is dependent on range and dispersion angle:

$$\sigma = \frac{\Theta_s R}{b} \qquad (22)$$

Clearly, it is desirable to eliminate aim bias and to reduce the intercept range to maximize the number of fragments impacting and hence the probability of kill.

In the initial case studied, where angle of attack equals zero and the missile velocity vector is assumed coincident with its heading, the required lead angle for

intercept (neglecting pellet drag effects) is given by:

$$\phi = \frac{V_T}{(V_M + V_{FIRE})} \sin \theta_T \qquad (23)$$

This is somewhat less than the required lead angle of the missile which is given by equation (17) (see figure 17). If the straight line collision course for predictive and proportional navigation has already been reached, the minimum time before impact to initiate the turn to come to this new lead angle can be approximated as:

$$t = \frac{V_m (\phi_m - \phi_F)}{n_L} \qquad (24)$$

where ϕ_m and ϕ_F are the required lead angles for the missile and fragments respectively, V_M is missile speed, and n_L is its lateral acceleration limits. For the more likely case where the missile is still turning to achieve a collision course, the terminal lateral acceleration demands are lessened as the required lead angle decreases to the necessary value at firing time. The effectiveness of pursuit navigation is even more dependent on the approach geometry. It was generally discovered that a missile using pursuit navigation was already accelerating at its limits to maintain the target at zero lead angle so that its effectiveness was limited to final approaches from head-on and from directly behind where required

fragment lead angles are minimum.

In trying to minimize the interception range, the missile's available turning rate and the LOS angular rate appear to be another limiting consideration. The LOS angular rate of rotation tends towards infinity as the missile approaches the target because it varies with the reciprocal of the range. The magnitude of LOS angular rate of change can be approximated by:

$$\dot{\Theta} \simeq \frac{V_T \sin \Theta_T}{R} \qquad (25)$$

The available turning rate of the missile is determined by its acceleration limit and quickly drops off with increasing velocity as seen in graph 4. The minimum range, therefore, that it is possible for a missile to follow the target's relative motion is given by:

$$R_{MIN} = \frac{V_M V_T \sin \Theta_T}{n_L} \qquad (26)$$

where V_T is target speed, Θ_T is target LOS angle, V_M is missile speed, and n_L is the lateral acceleration limit of the missile. While it may still be possible to hit the target at less than this range with favorable geometry, it becomes impossible for the missile to lead the target at the proper angle beyond this point.

When aerodynamic effects are introduced and the angle

of attack no longer equals zero, the problem is greatly complicated. Aiming considerations are then shifted to controlling missile attitude immediately before firing. This aim angle can be derived from final engagement geometry (figure 10) but must be solved for iteratively because of the extreme non-linear nature of the equations which also take pellet drag into account. While the desired instantaneous lead angle can be determined it is not quite clear at this time how to effectvely implement final alignment of the missile taking all of the aerodynamic factors described in the aerodynamic transfer function into account.

VI. CONCLUSION AND SUMMARY

This study successfully modelled many of the parameters which characterize missile dynamics, hypervelocity flight, and projected performance of the Directed Energy Projectile Weapon. While specific analysis will have to wait until an actual weapon is designed, this work establishes some of the performance criteria which will prove critical in producing an effective weapon and provides a useful tool for studying design trade-offs.

Computer simulation using the MISDYN code developed with ACSL (Advanced Continuous Simulation Language) and FORTRAN, validated the basic premise of the concept using a non-aerodynamic effect model. For a general set of initial conditions both proportional and predictive navigation proved effective in getting the missile into a favorable attack geometry at which time a predictive fuze could be used for final alignment and firing. Pursuit navigation proved to be of limited but effective use for only a small number of favorable initial conditions. This analysis shows that there are no other physical limitations that would preclude system effectiveness outside of the dynamic response which has not yet been evaluated. As previously stated, the inclusion of the aerodynamic transfer function complicates matters

significantly. While at this time a simple solution does not appear available, there is no reason to believe a workable scheme can not be developed with further study.

Warhead effectiveness will ultimately depend on design parameters, particularly mass issues. The warhead itself has been shown to be capable of producing the required lethality levels given reasonable design parameters.

Overall preliminary system's analysis finds no insurmountable obstacles at this level, assuming that warhead efficiencies can be raised to an acceptable level, and recomends future development. This system has the potential to revolutionize current anti-air capabilities by increasing lethality at ranges several magnitudes greater than those currently available.

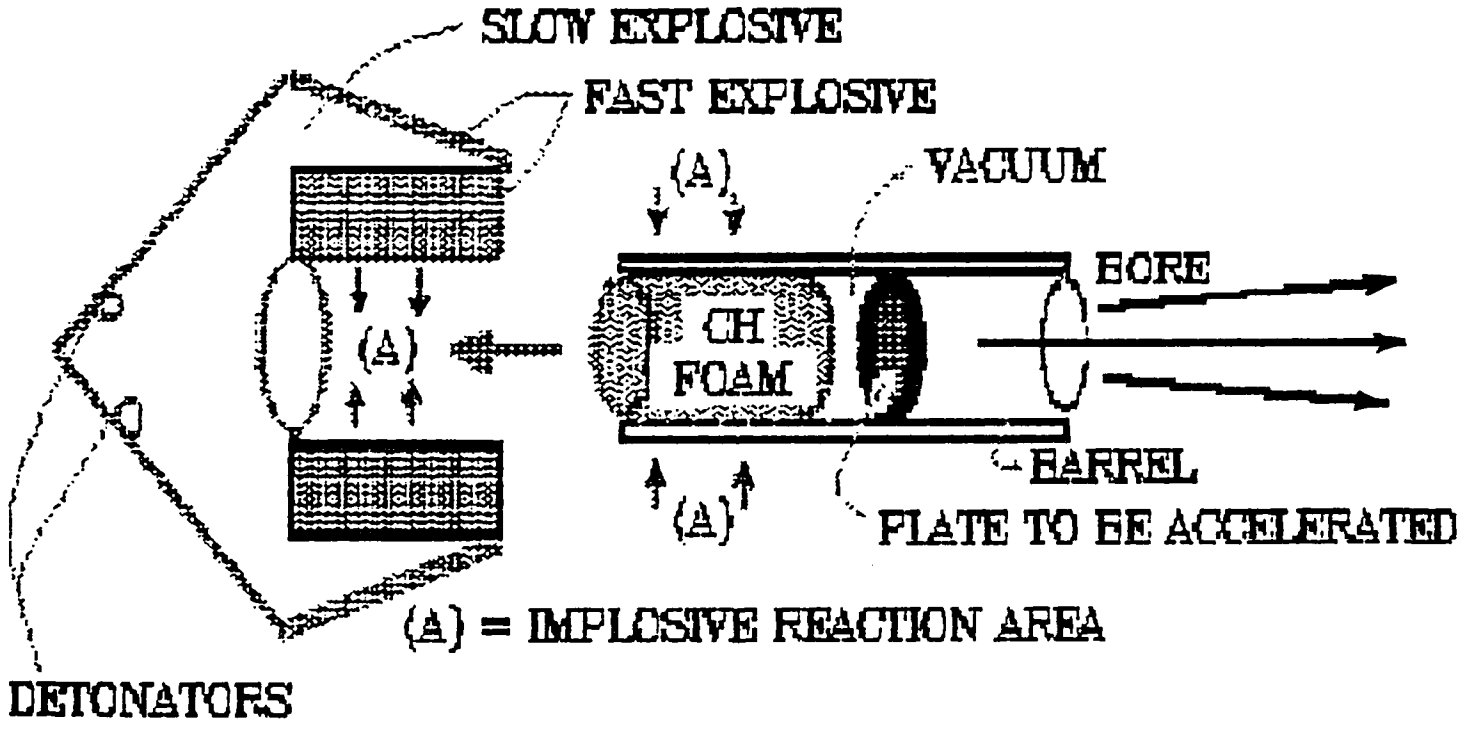

FIG 1. IMPLODING LENS WARHEAD AND SHOCKTUBE

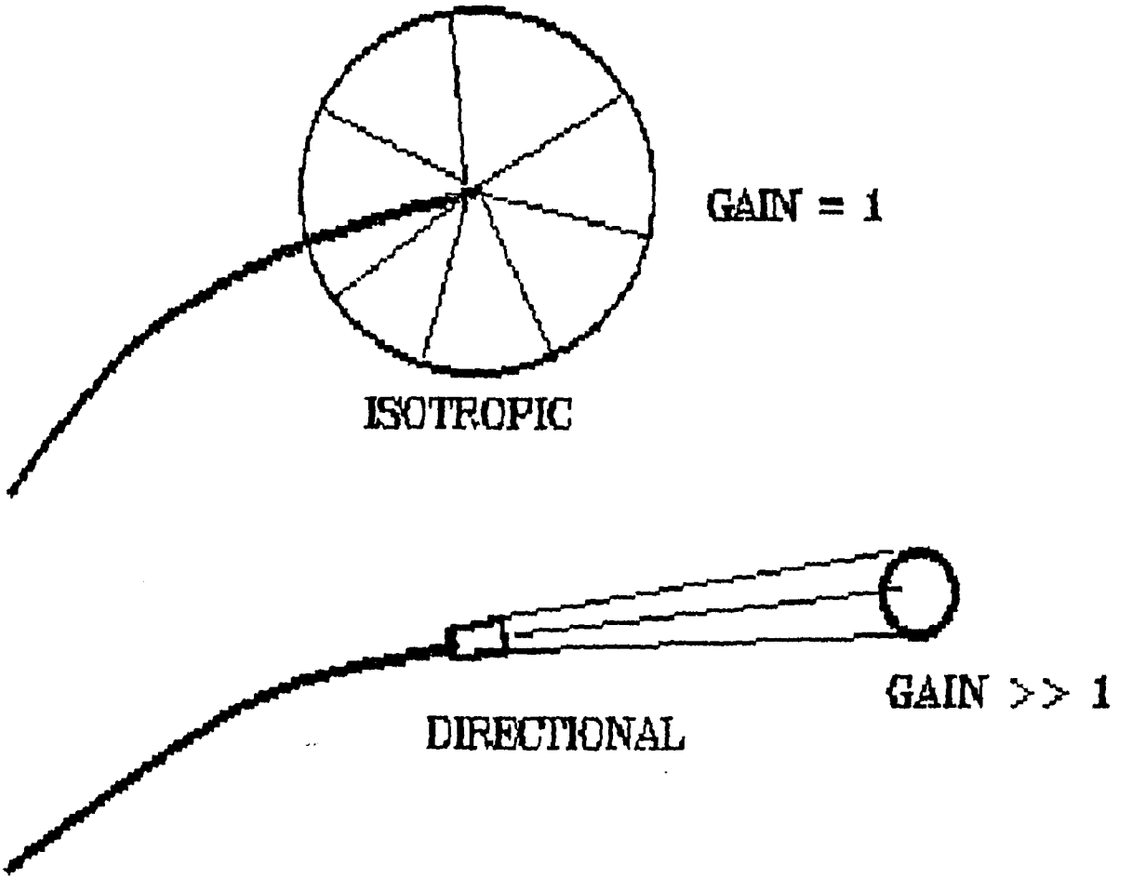

$$\text{WARHEAD GAIN} = \frac{\text{SURFACE AREA OF SPHERE}}{\text{SURFACE AREA OF DISK}}$$

FIG 2. WARHEAD GAIN

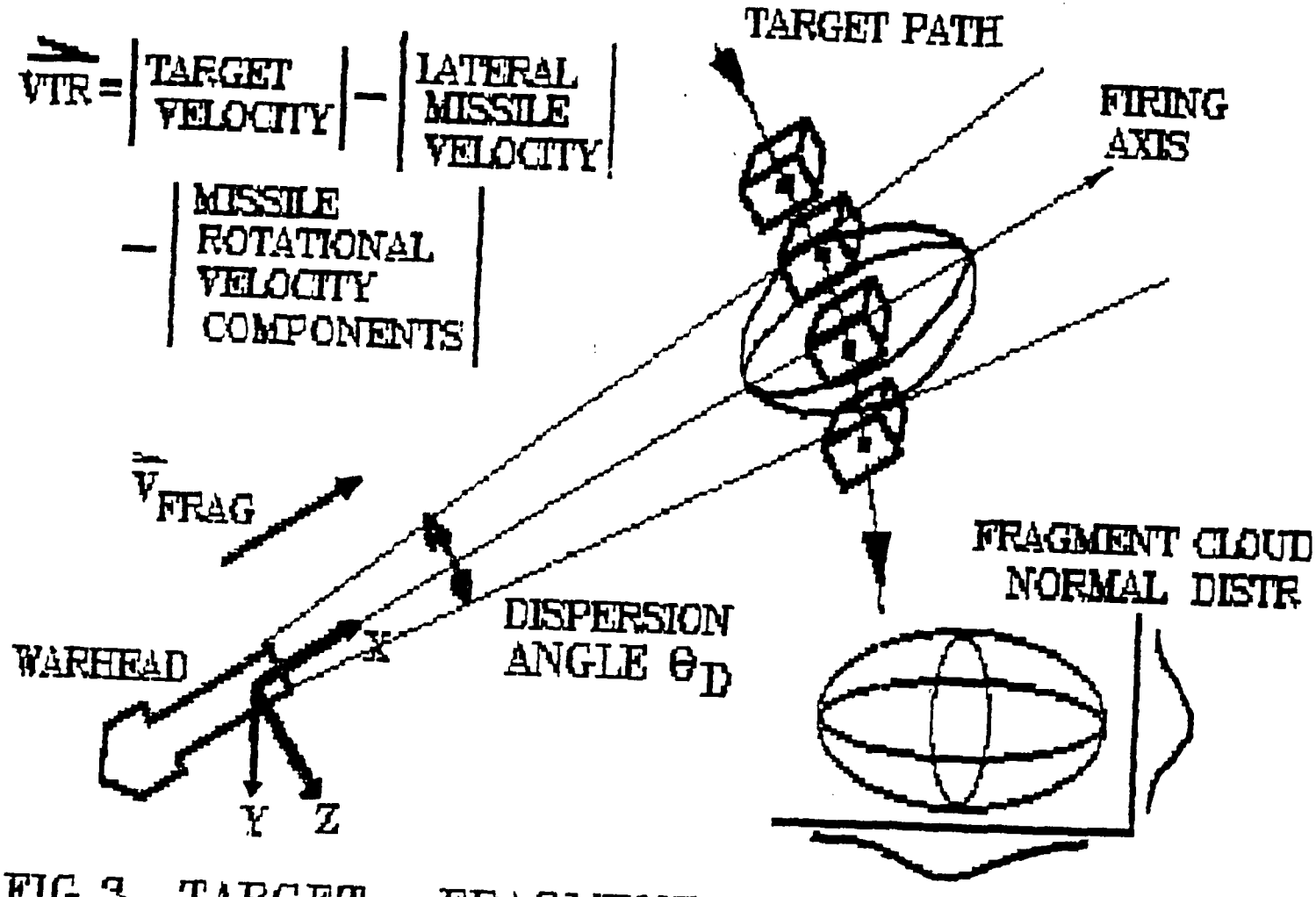

FIG 3. TARGET – FRAGMENT CLOUD INTERACTION

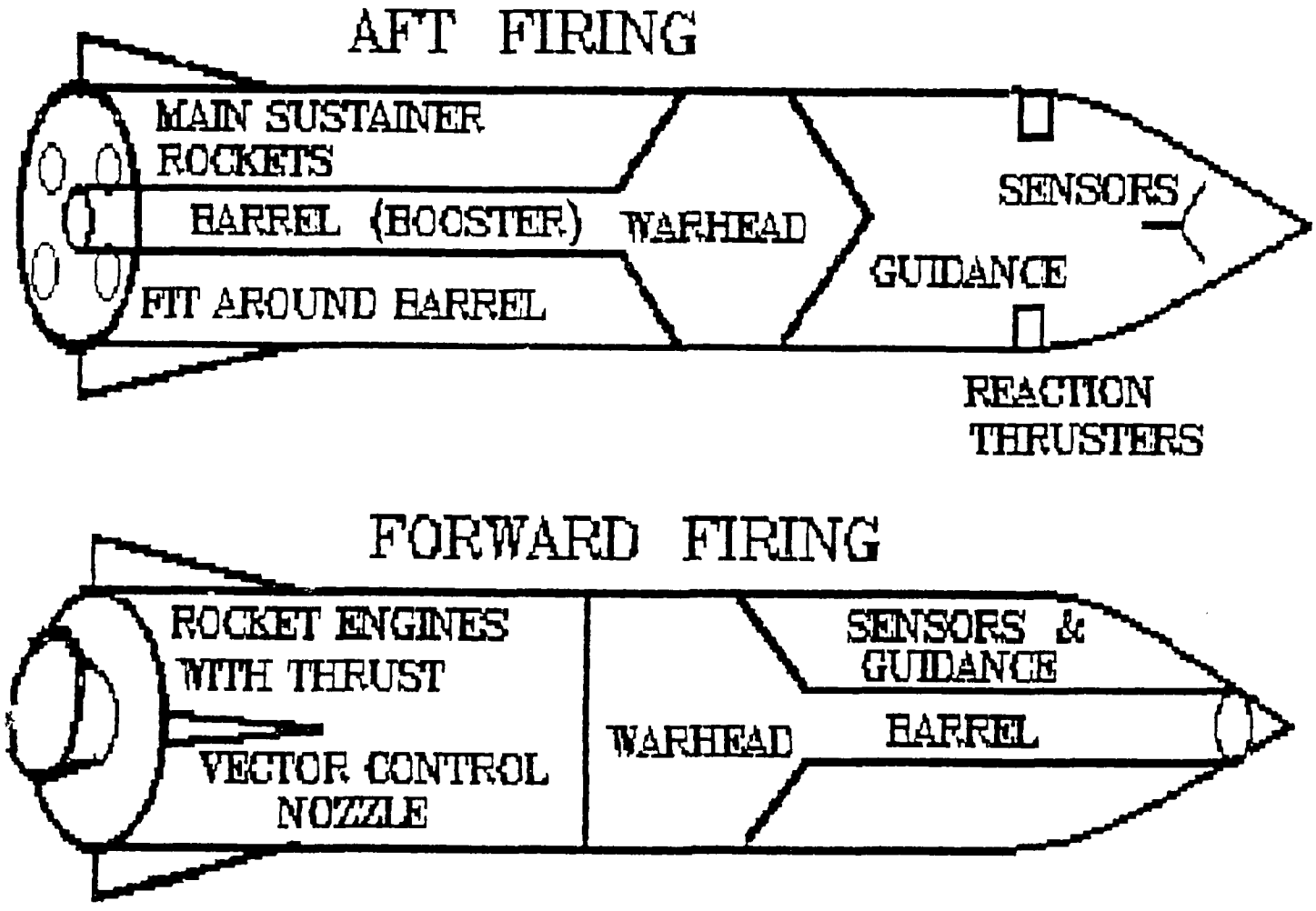

FIG 4. ROCKET CONFIGURATIONS

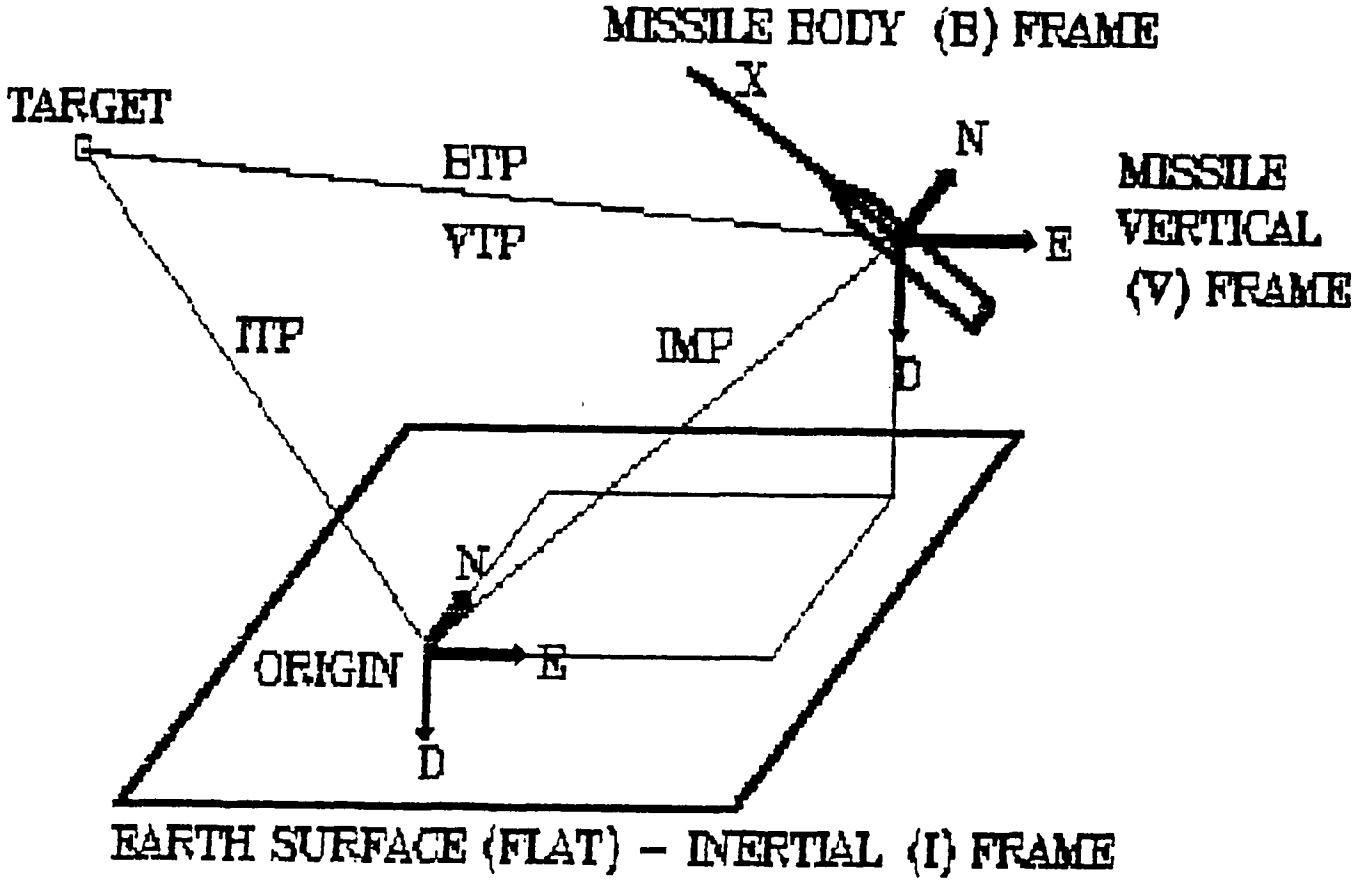

FIG 5. COORDINATE SYSTEMS

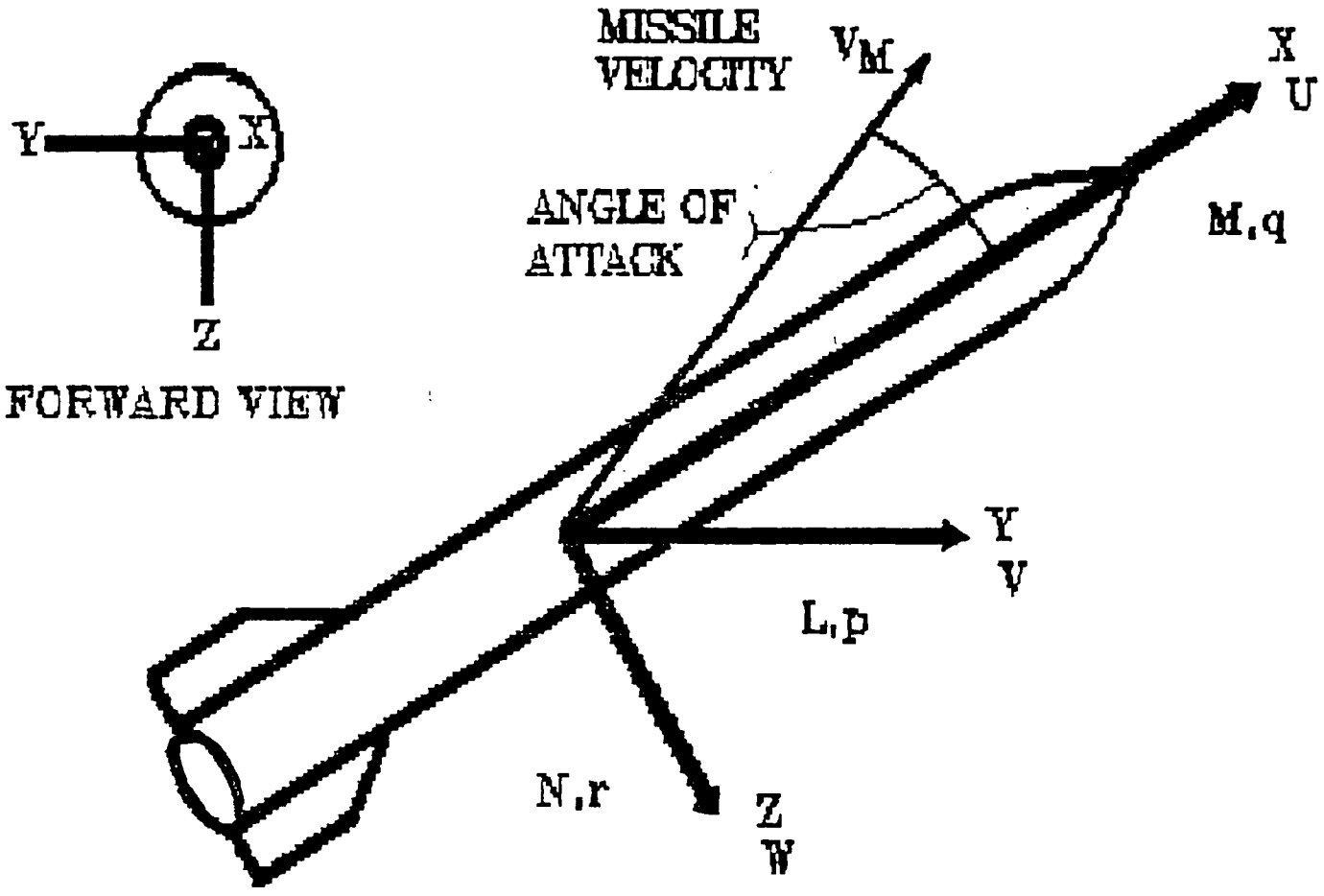

FIG 6. MISSILE BODY AXES & REFERENCE FRAME

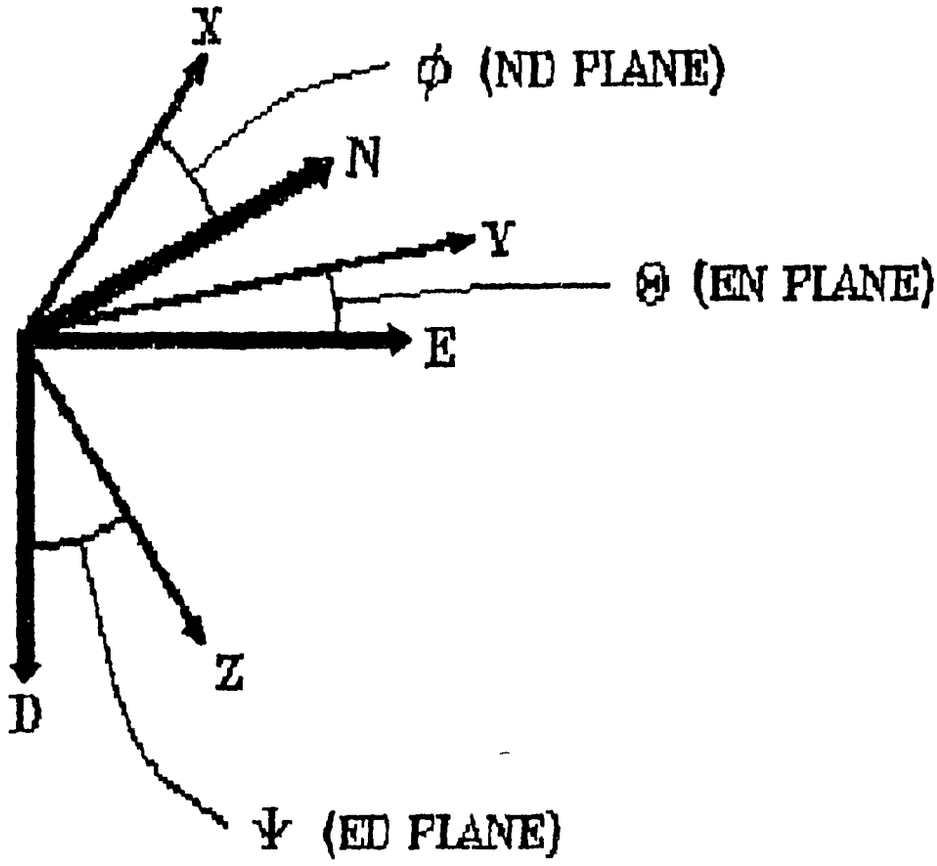

FIG 7. EULER ROTATION ANGLES

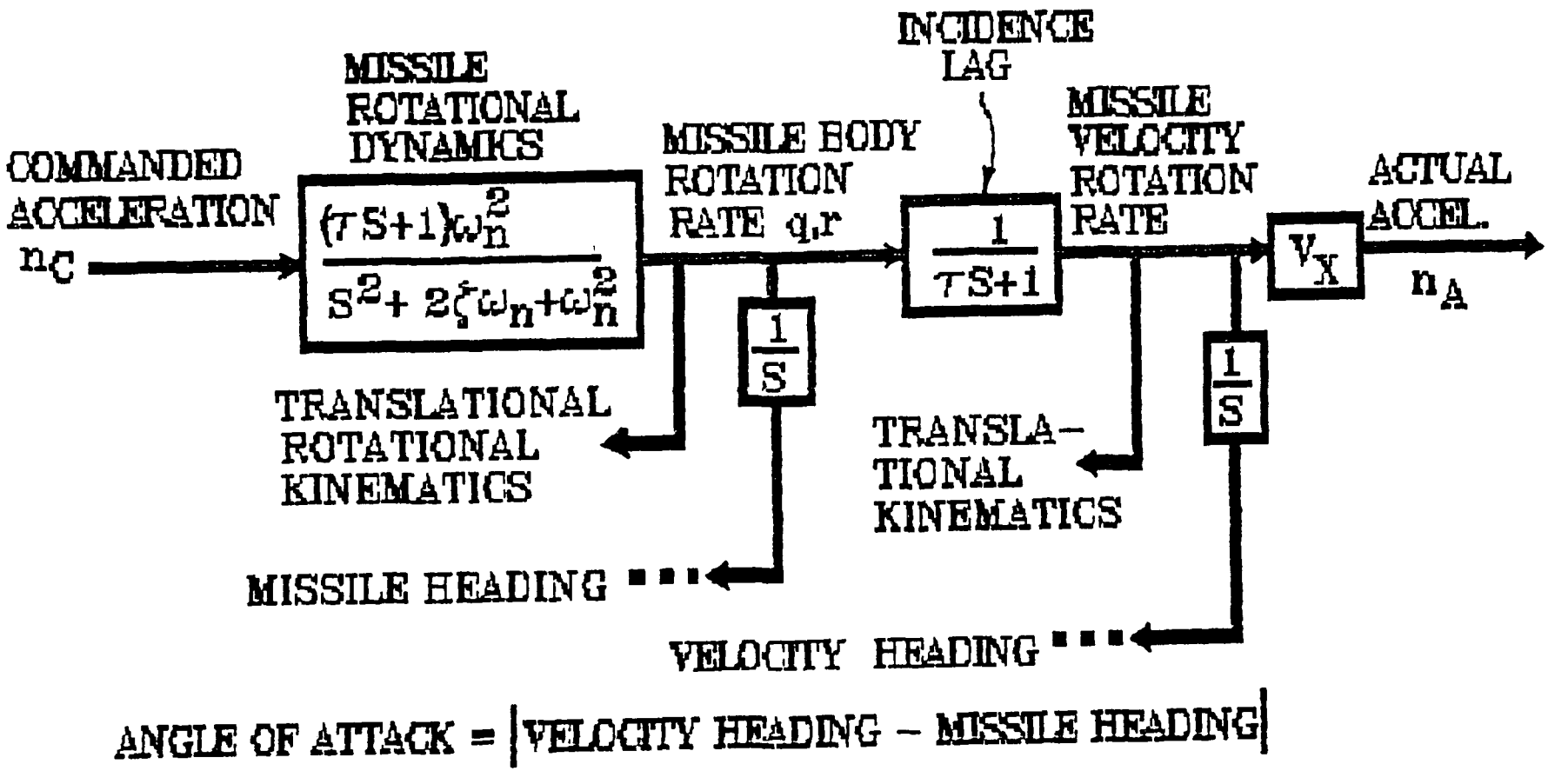

FIG 8. AERODYNAMIC TRANSFER FUNCTION

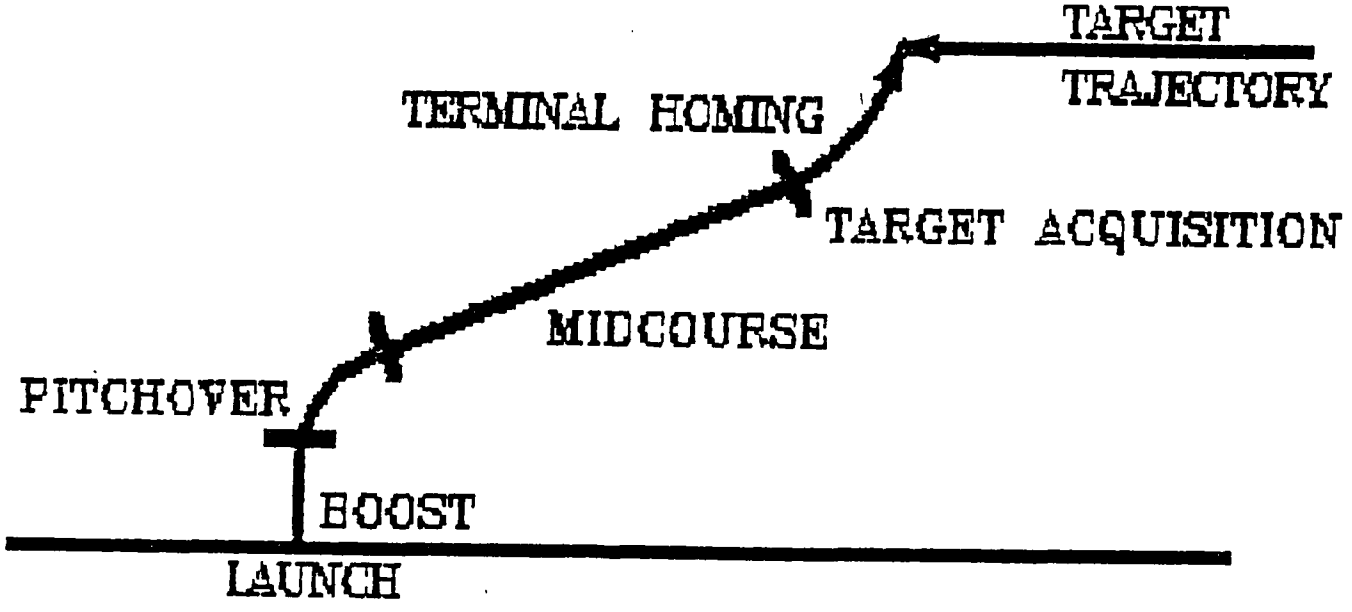

FIG 9. MISSILE FLIGHT PHASES

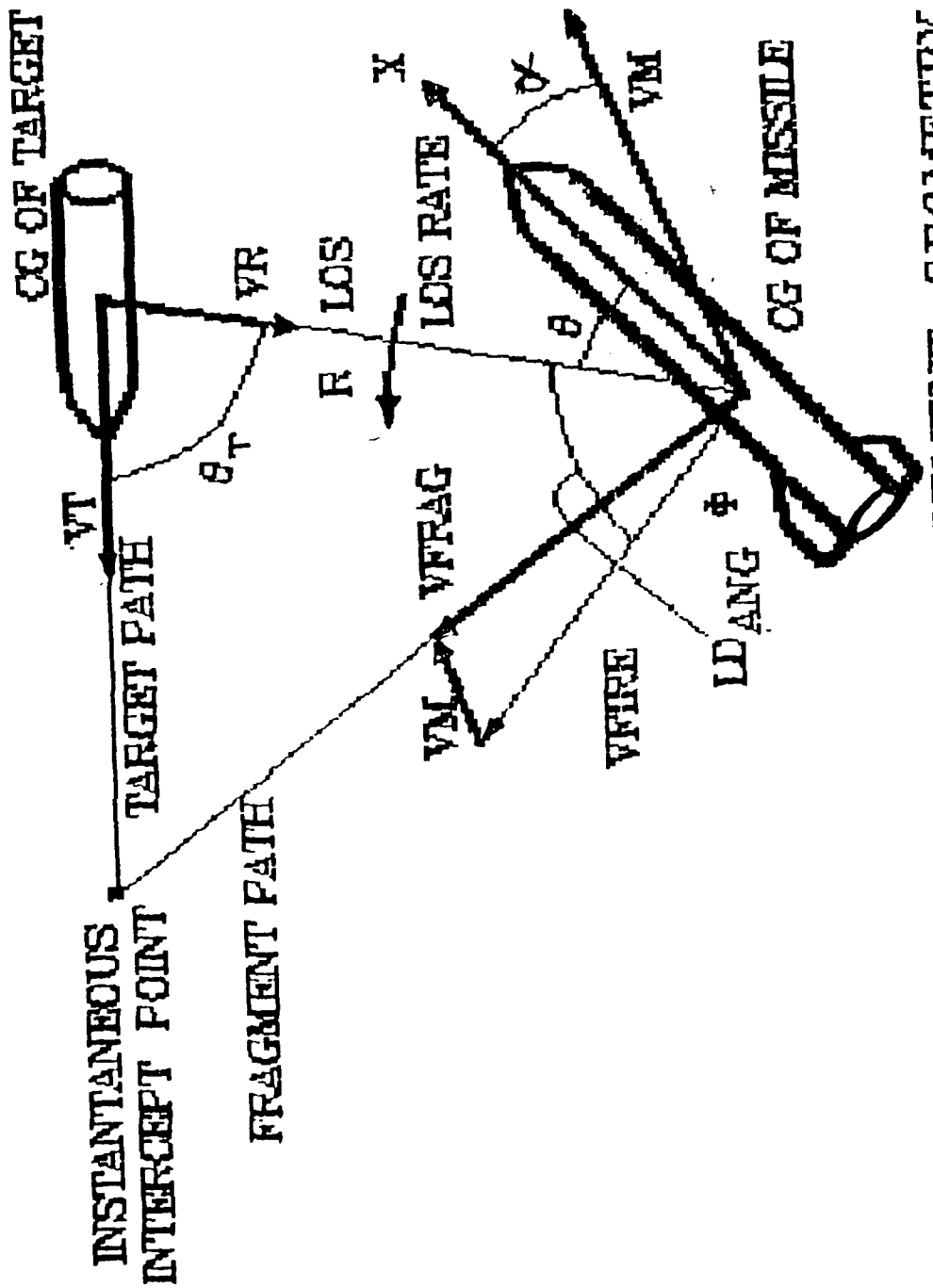

FIG 10. TERMINAL ENGAGEMENT GEOMETRY

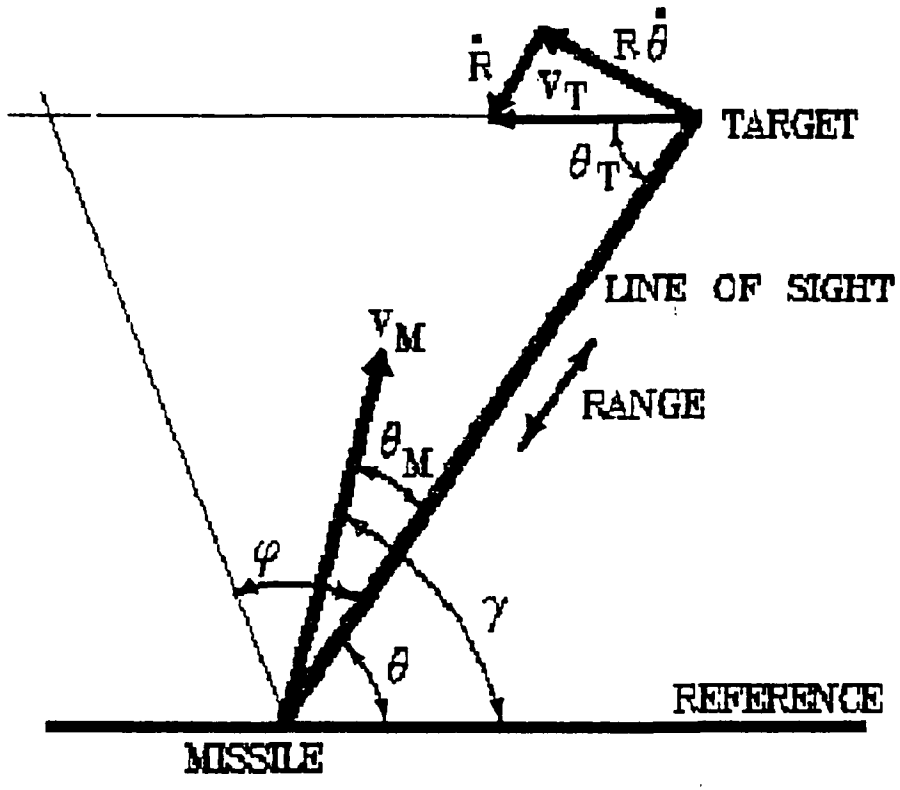

θ_T – TARGET LOS ANGLE

θ_M – MISSILE LOS ANGLE

γ – MISSILE FLIGHT PATH ANGLE

θ – REFERENCE LOS ANGLE

φ – LEAD ANGLE

$\dot{R}$ – LOS RANGE RATE

$R\dot{\theta}$ – TANGENTIAL VELOCITY

FIG 11. GUIDANCE GEOMETRY

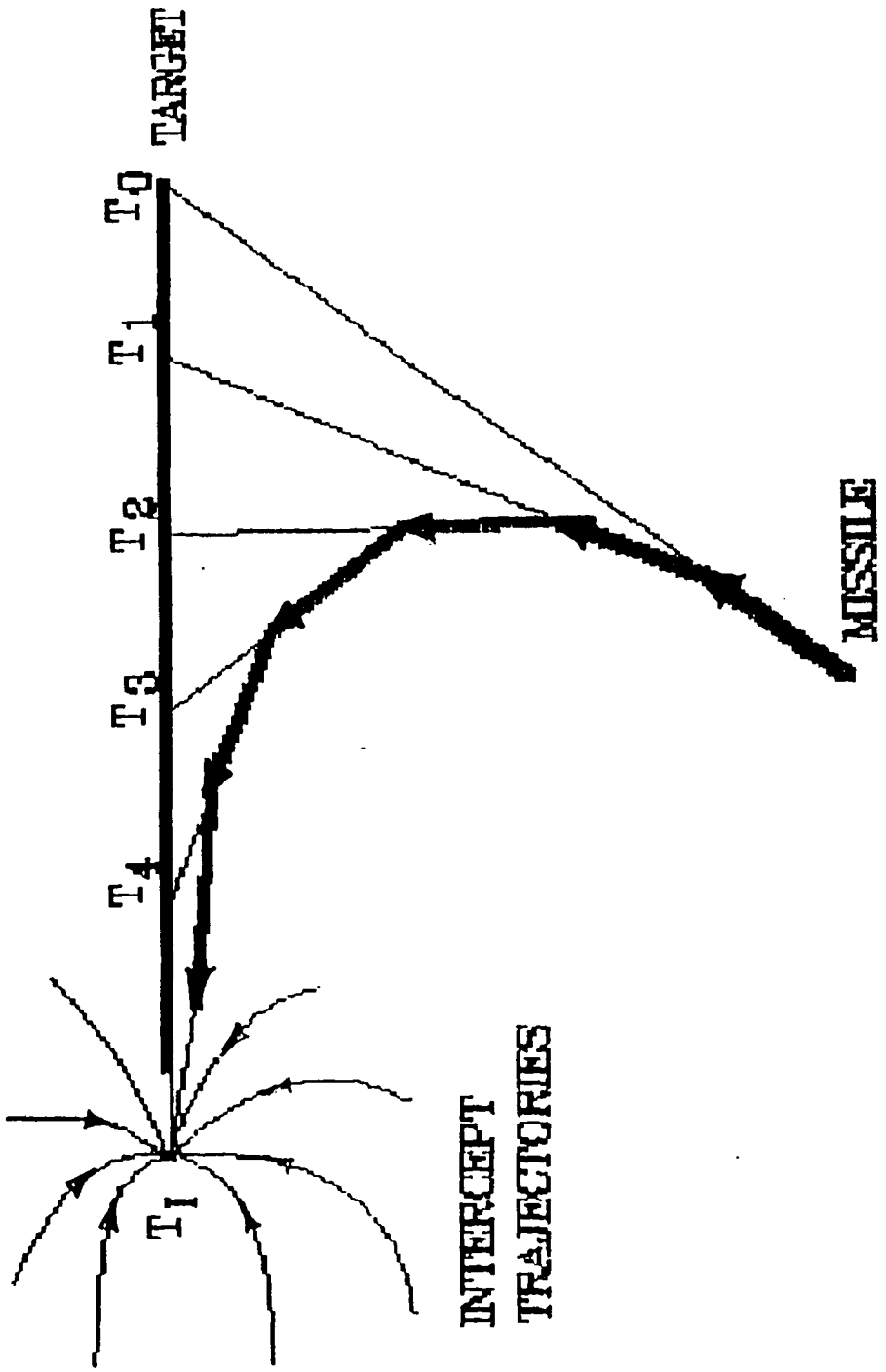

FIG 12. PURSUIT GUIDANCE

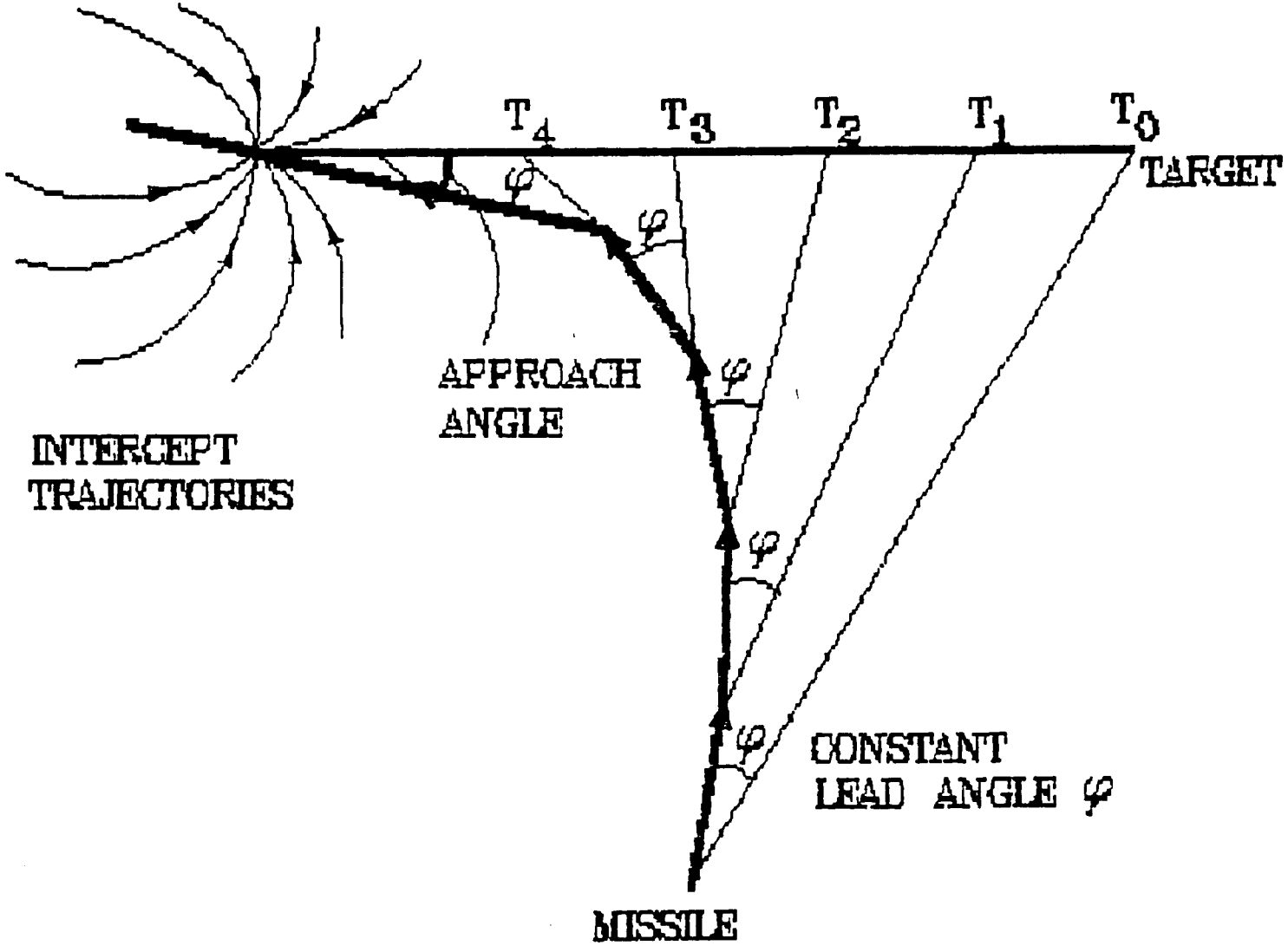

FIG 13. LEAD ANGLE GUIDANCE

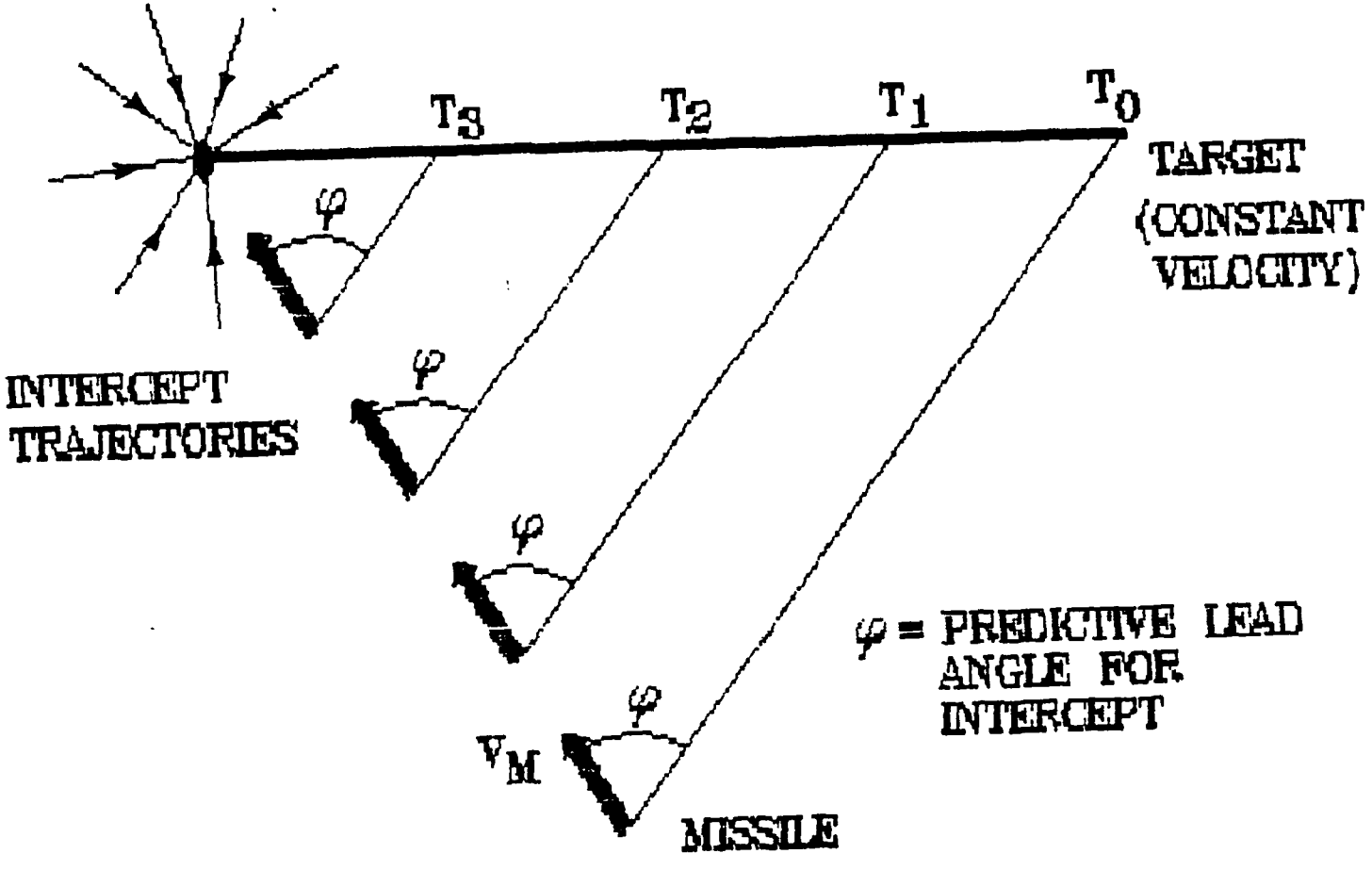

FIG 14. PREDICTIVE GUIDANCE

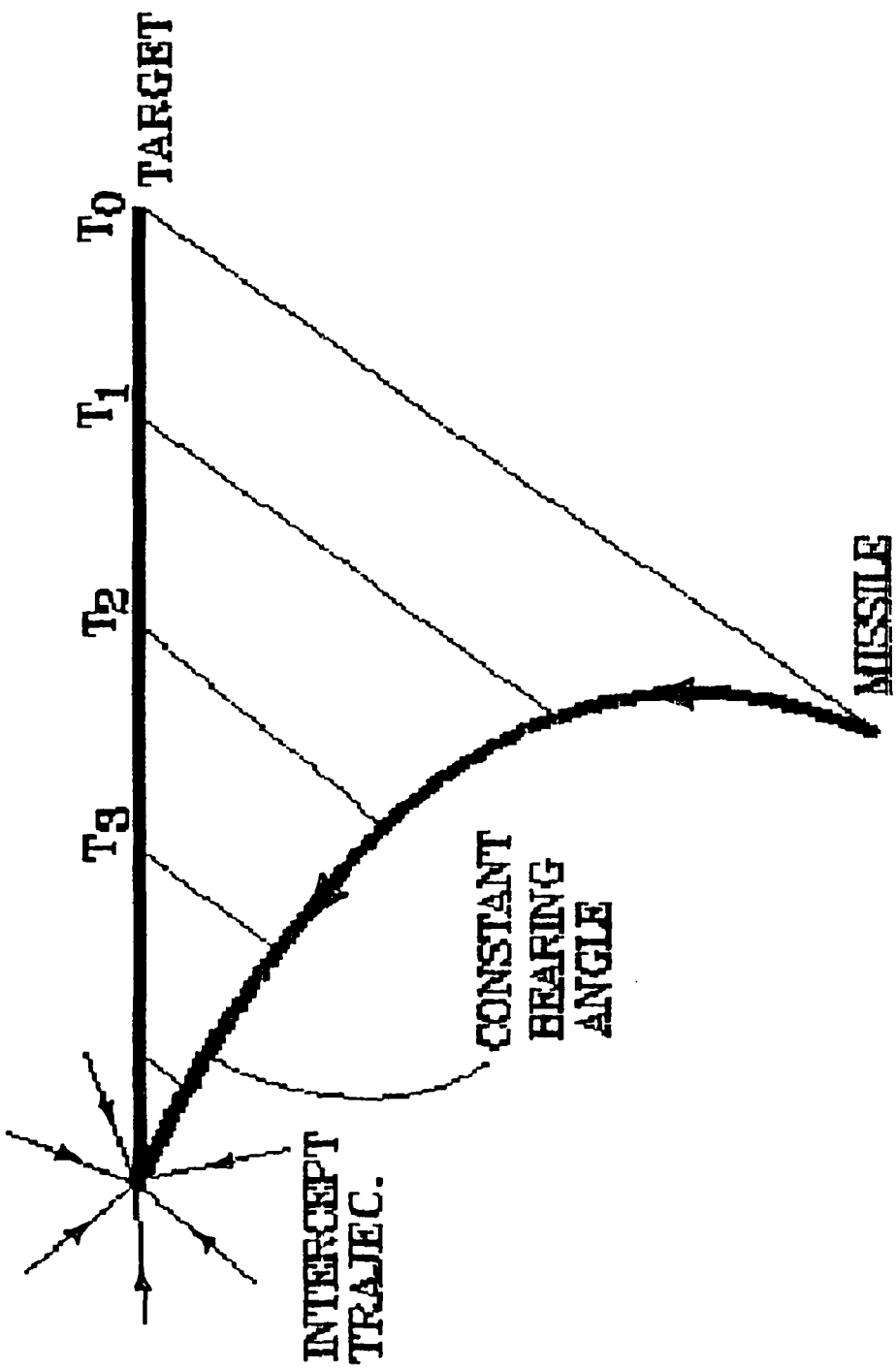

FIG 15. PROPORTIONAL NAVIGATION

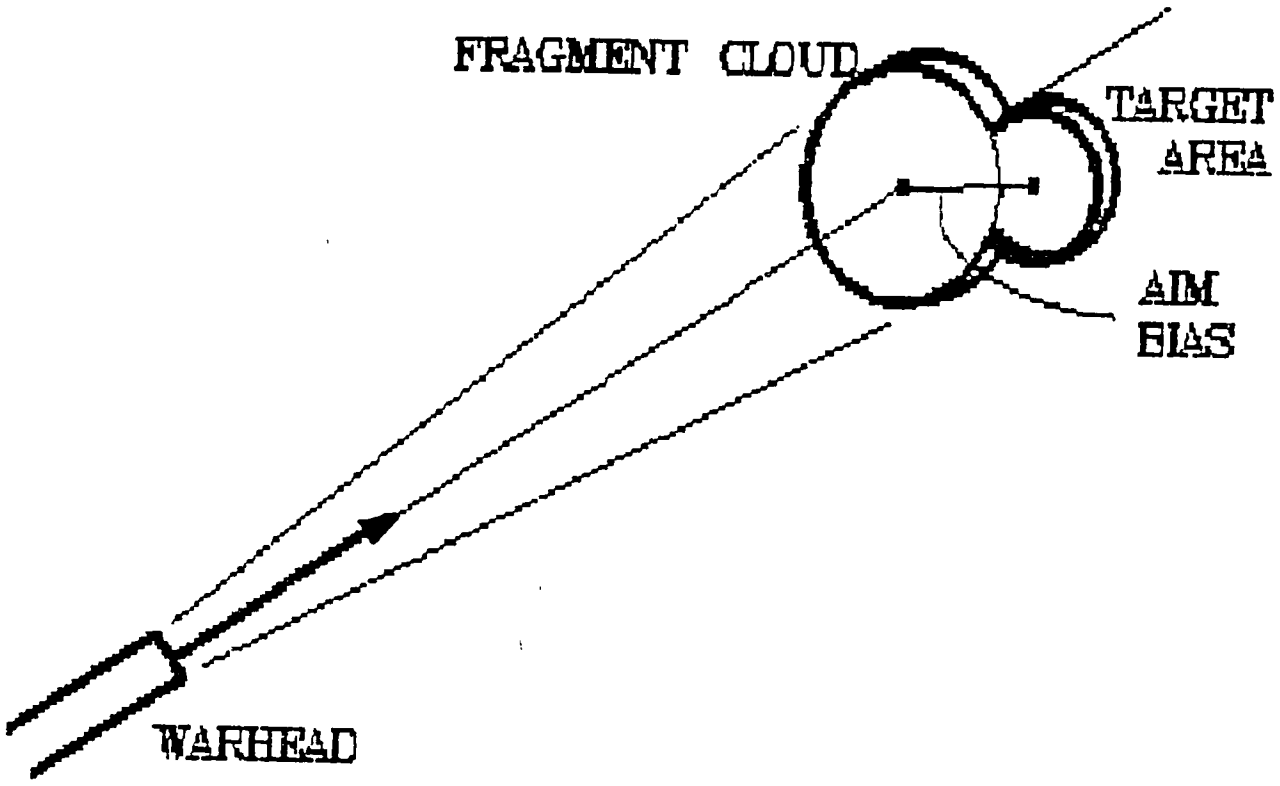

FIG 16. FRAGMENT KILL GEOMETRY

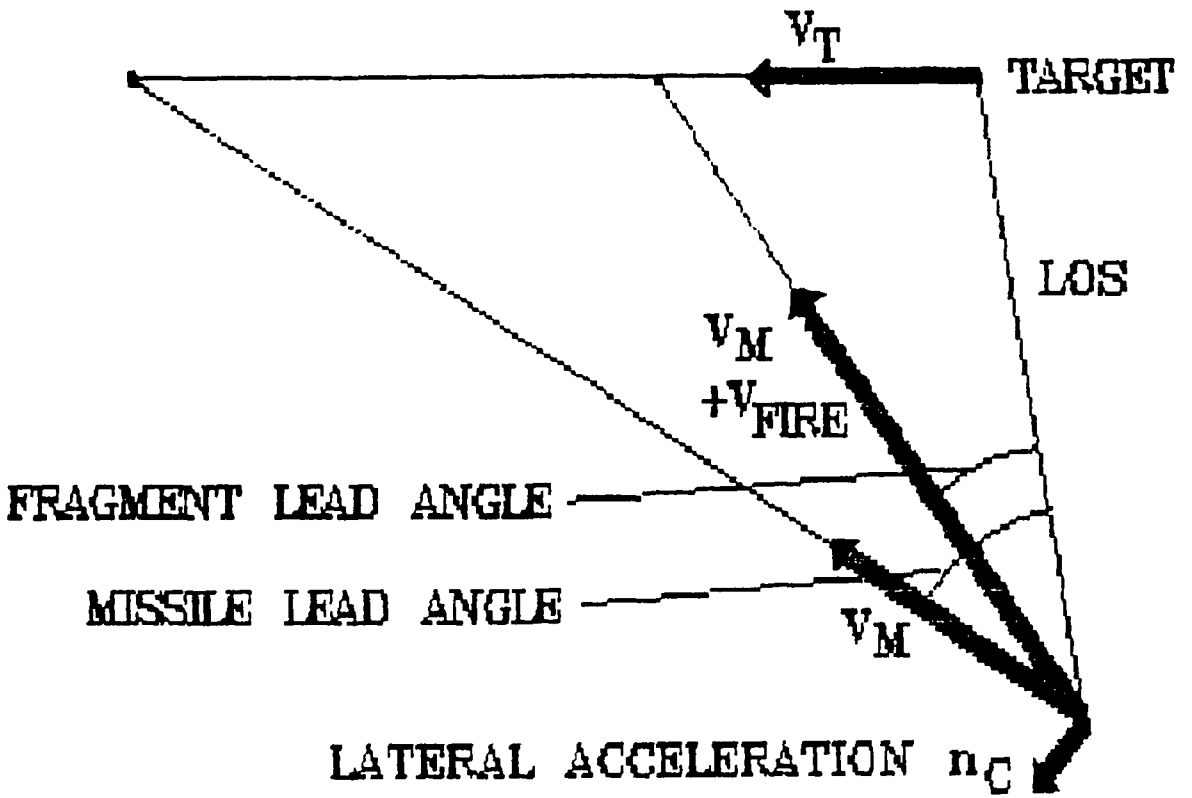

FIG 17. FRAGMENT FIRING GEOMETRY

TABLE 1. WARHEAD GAIN

DISPERSION ANGLE θ_D DEGREES	GAIN
0.0	∞
0.5	210000
1.0	52500
1.5	23400
2.0	13100
2.5	8400
3.0	5800
3.5	4300
4.0	3300
4.5	2600
5.0	2100
6.0	1500
7.0	1100
8.0	820
9.0	650
10.0	144

$$\text{GAIN} = \frac{16}{\theta_D^2} \qquad \text{WITH } \theta_D \text{ IN RADIANS}$$

TABLE 2. VELOCITY AND KINETIC ENERGY RELATIONSHIP

MASS = 1.0 G.

VELOCITY (KM/S)	KINETIC ENERGY (JOULES)
0.5	125
1.0	500
1.5	1125
2.0	2000
2.5	3125
3.0	4500
4.0	8000
5.0	12500
6.0	18000
7.0	24500
8.0	32000
9.0	40500
10.0	50000
11.0	60500
12.0	72000

$$K.E. = 0.5\ MV^2$$

TABLE 3. LETHALITY RESULTS

Lethality Figure of Merit for 75 1.0 gram Tungsten Pellets against 1/2 square meter Target at 10.0 km altitude with a five degree dispersion angle

Initial Velocity (km/s)	Figure of Merit (newtons)	Required Gain
	Range = 100.0 m	
5.0	12,596	79.4
7.5	28,623	34.9
10.0	51,505	19.4
	Range = 50.0 m	
5.0	61,357	16.3
7.5	137,909	7.3
10.0	235,959	4.2
	Range = 25.0 m	
5.0	143,633	7.0
7.5	326,718	3.1
10.0	552,099	1.8

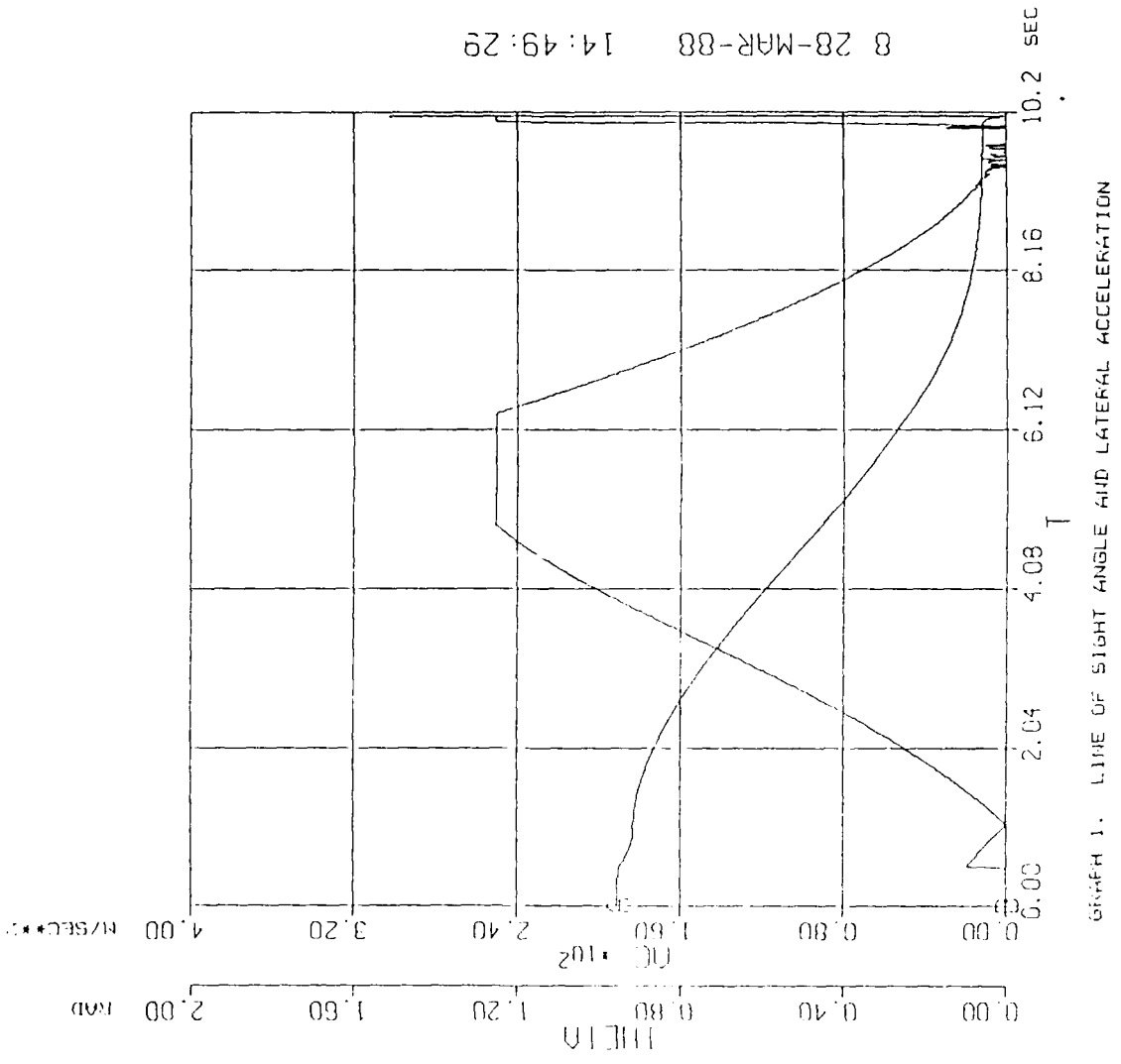
8 28-MAR-88 14:49:29
0.00
2.04
4.08
6.12
8.16
10.2
SEC
T
LINE OF SIGHT ANGLE AND LATERAL ACCELERATION

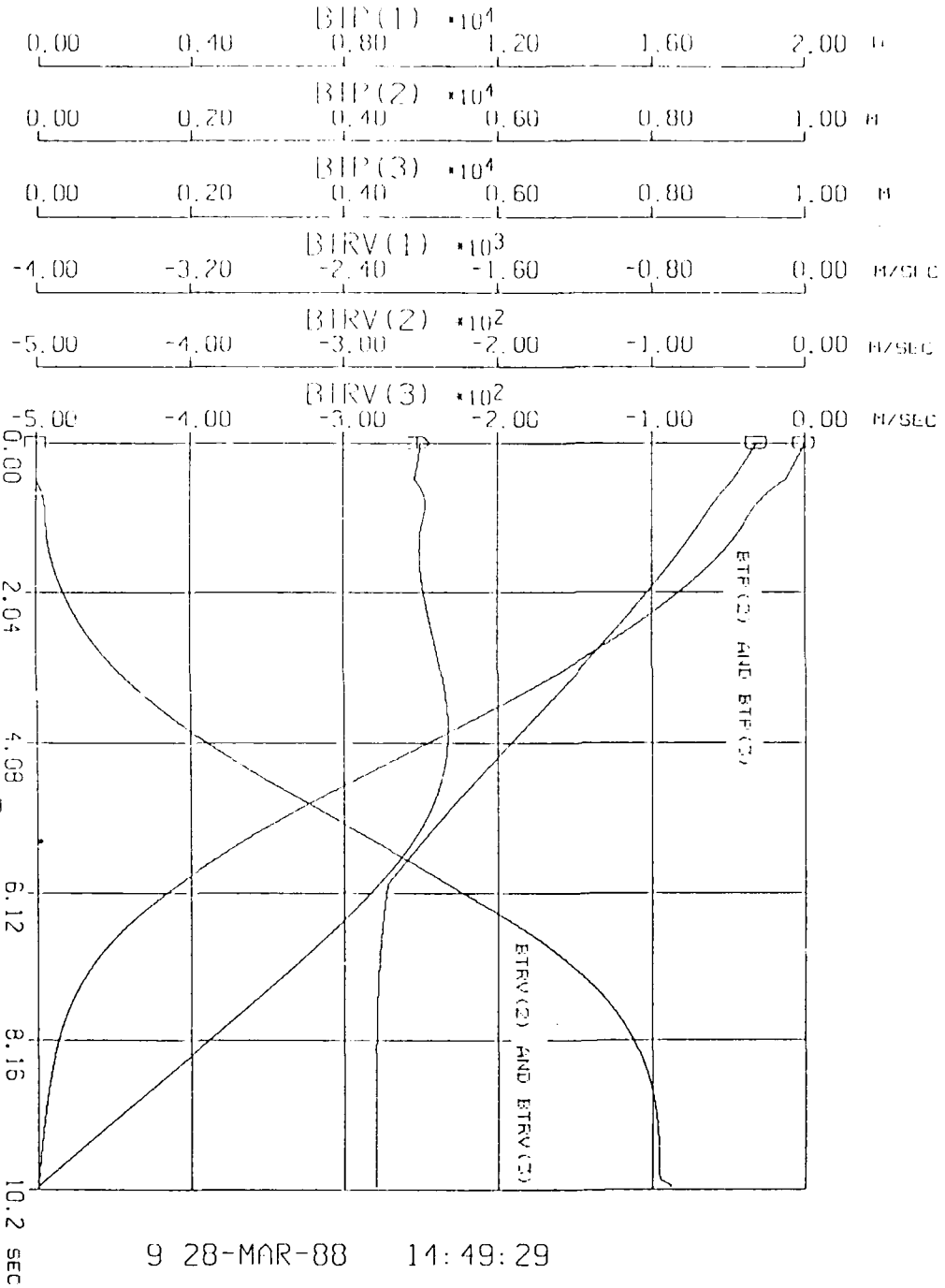

GRAPH 2. TARGET'S RELATIVE POSITION AND VELOCITY

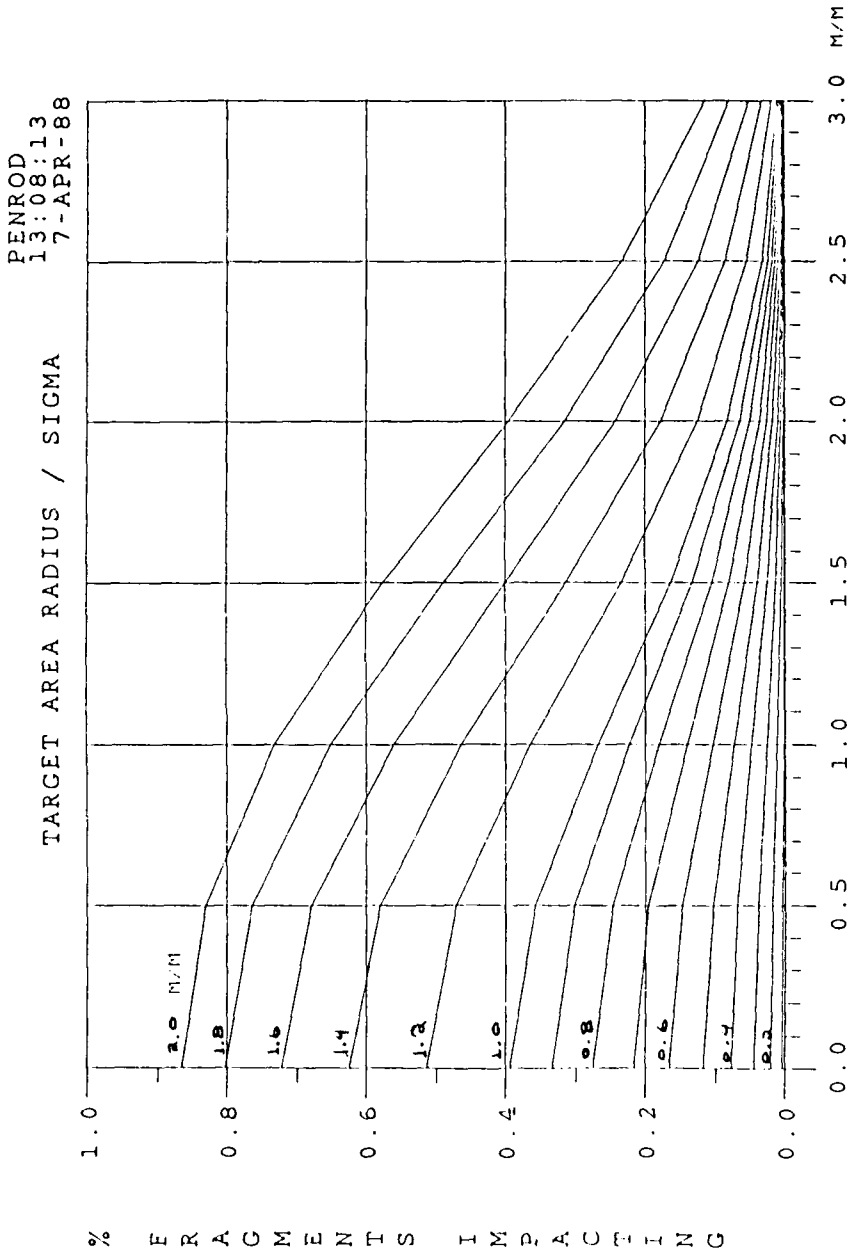

GRAPH 3. EFFECT OF MISS DISTANCE ON PERCENT FRAGMENTS IMPACTING

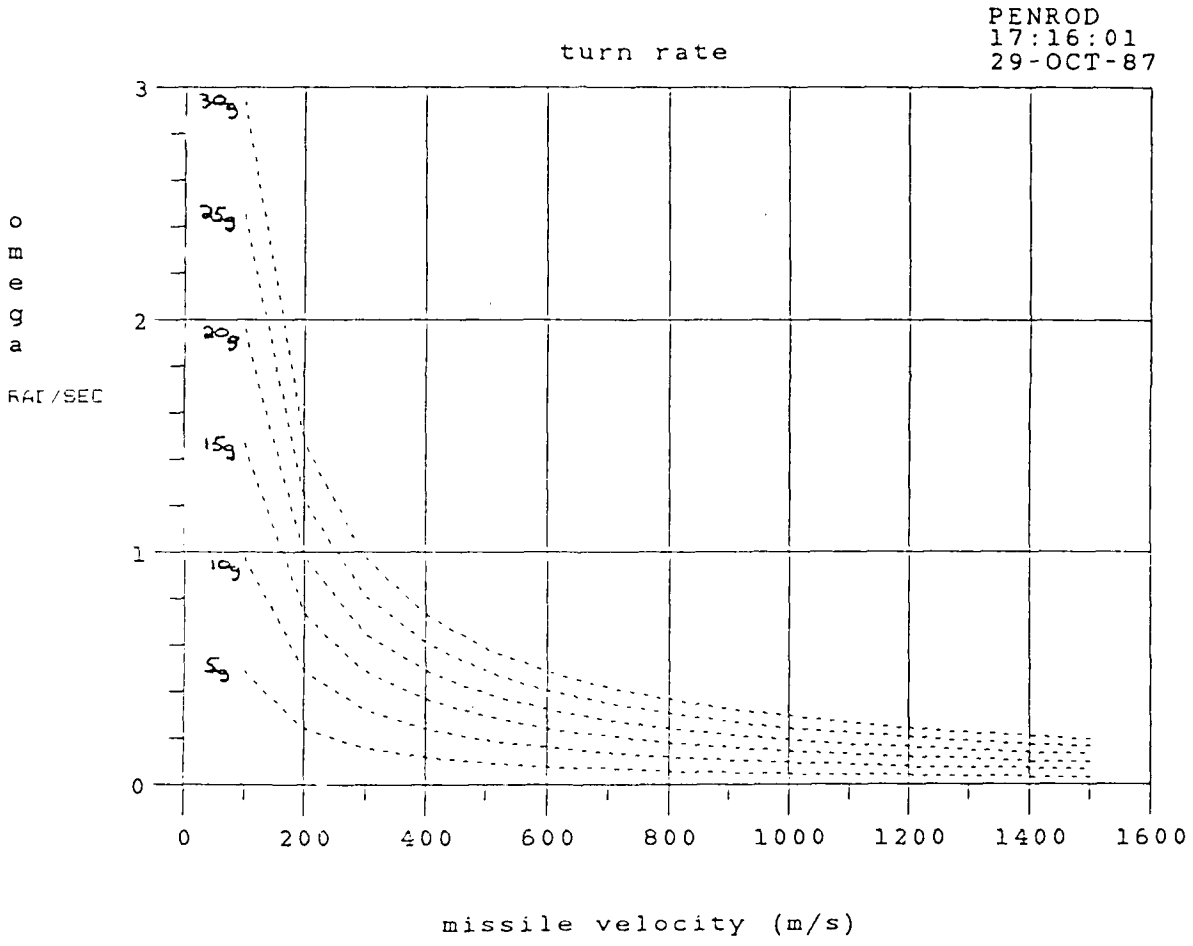

GRAPH 4. LATERAL ACCELERATION LIMITS VERSUS VELOCITY

REFERENCES

1. McCall,Gene H.,"A Method for Producing Shockless Acceleration of Masses to Hypervelocities Using High Explosives", La Jolla Institute Report, LJI-TM-84-106, 1984.

2. Unpublished manuscript on "Pellet Transport through the Atmosphere" prepared for Los Alamos National Laboratory by SAIC, 1987.

3. Held, M.,"Warheads for SAM Systems", AGARD Lecture Series No. 135, 1984.

BIBLIOGRAPHY

Bonds,R., Advanced Technology Warfare, (Salamander Books, Ltd.,London, 1985).

Burington,R.S. and May,D.C., Handbook of Probability and Statistics with Tables,(McGraw-Hill,Inc., New York, 1970).

Etkin,Bernard ,Dynamics of Atmospheric Flight, (John Wiley & Sons, Inc., 1972).

Cummings,P., DeMuth,N., Penrod,S. and Saylor,W., "DEPW Implications for Missile Design", unpublished notes from Los Alamos National Laboratory, 1987.

Forrest,K.M.,FLTLT,RAAF, "Production of a Digital Computer Simulation of the Trajectory of a Thrust Vector Controlled Air to Air Missile in Three Dimensions" , M.S. Thesis, Loughborough University of Technology RAF College - Cranwell, 1985.

Frieden,D.R., Principles of Naval Weapons Systems, (Naval Institute Press, Annapolis,Md, 1985).

Garnell,P. and East,D.J., Guided Weapons Control Systems, (Pergamon Press, Oxford, 1977).

Held,M.,"Warheads for SAM Systems", AGARD Lecture Series No.135, 1984.

Jerger,J.J., Systems Preliminary Design, Principles of Guided Missile Design,(D. Van Nostrand Company Inc., Princeton, 1960).

Kim,Y.S., Cho,H.S., and Bien,Z., "A New Guidance for Homing Missiles" , Journal of Guidance and Control, Vol. 8, No.3, 1985, pp. 402-404.

Locke,A.S., Guidance, Principles of Guided Missile Design, (D. Van Nostrand Company, Inc.,Princeton, 1955).

McCall,G.H., "A Method for Producing Shockless Acceleration of Masses to Hypervelocities using High Explosives", LaJolla Institute Report, LJI-TM-64-106, 1984.

Mitchell and Gauthier Associates, Advanced Continuous Simulation Language (ACSL) REFERENCE MANUAL, USA, 1986.

SAIC, "Pellet Transport Through the Atmosphere", Los Alamos National Laboratory, 1987.

Wertz,J.R., Spacecraft Attitude Determination and Control, (D. Reidel Publishing Company, Dordecht, Holland, 1978)

APPENDIX A. DRAG EQUATIONS

By equating Newton's force equation, F=mA, to equation (2) which describes the atmospheric drag forces, drag deceleration, A_D, can be solved as:

$$A_D = \frac{dV}{dt} = -\frac{1}{2} \rho_\infty V^2 \frac{A_p}{m} C_D \qquad \text{(A-1)}$$

where ρ_∞ is atmospheric density, V is velocity, A_p is projected area, m is mass, and C_D is the coefficient of drag. By assuming that ρ_∞ ,the atmospheric density,which can be estimated from altitude, ALT, as:

$$\rho_\infty \simeq 1.752 \; e^{-\left(\frac{ALT}{6100}\right)} \qquad \text{(A-2)}$$

is constant over the short flight distances prescribed, and given that the terms A_p/m and C_D are constant in the no ablation continuum flc. region, it is possible to define a drag constant ,S_0:

$$S_o = \frac{2}{\rho_\infty C_D} \left(\frac{m}{A_p}\right) \qquad \text{(A-3)}$$

so that the acceleration can be given as:

$$A_D = \frac{dV}{dt} = -\frac{V^2}{S_o} \qquad \text{(A-4)}$$

Which can be integrated with respect to v and rearranged to yield velocity as a function of initial velocity, V_0, and time of flight, t:

$$V = \frac{V_0 S_0}{V_0 t + S_0} \qquad \text{(A-5)}$$

Using the identity:

$$\frac{1}{V} \frac{dv}{dt} = \frac{dv}{ds} \qquad \text{(A-6)}$$

and then integrating, the distance a pellet travels in time, t, when slowed by drag can be found to be:

$$S = S_0 \ln\left(\frac{V_0 t}{S_0} + 1\right) \qquad \text{(A-7)}$$

Graph A1 shows lines of constant S_0 value as they vary with mass and altitude for spherical tungsten pellets. Physically the term S_0 corresponds to the range where the velocity has slowed by a factor of e (2.718). The smallest values of S0 which correspond to the shortest effective ranges are found in the lower left of the graph where mass and altitude are minimum. S_0 increases with both altitude and mass making for longer effective ranges. It should be noted that mass and altitude are only parameters for pellet radius and atmospheric density which are the true

parameters effecting drag. Graphs A2 through A5 display the effects of S_0 on range and final velocity given the initial fragment velocity and time of flight. Each graph represents values at at a specific instant in time after firing. The negative sloping curves represent ccnstant values of final velocity. The positive sloping curves represent the distance the pellet has travelled in 10 meter increments starting with 10 meters on the bottom curve and 150 on the top which can be considered the effective engagement range. As the time after firing increases the engagement range moves down the initial velocity scale and the value of the final velocity curves given on the right hand of the graph decrease as expected.

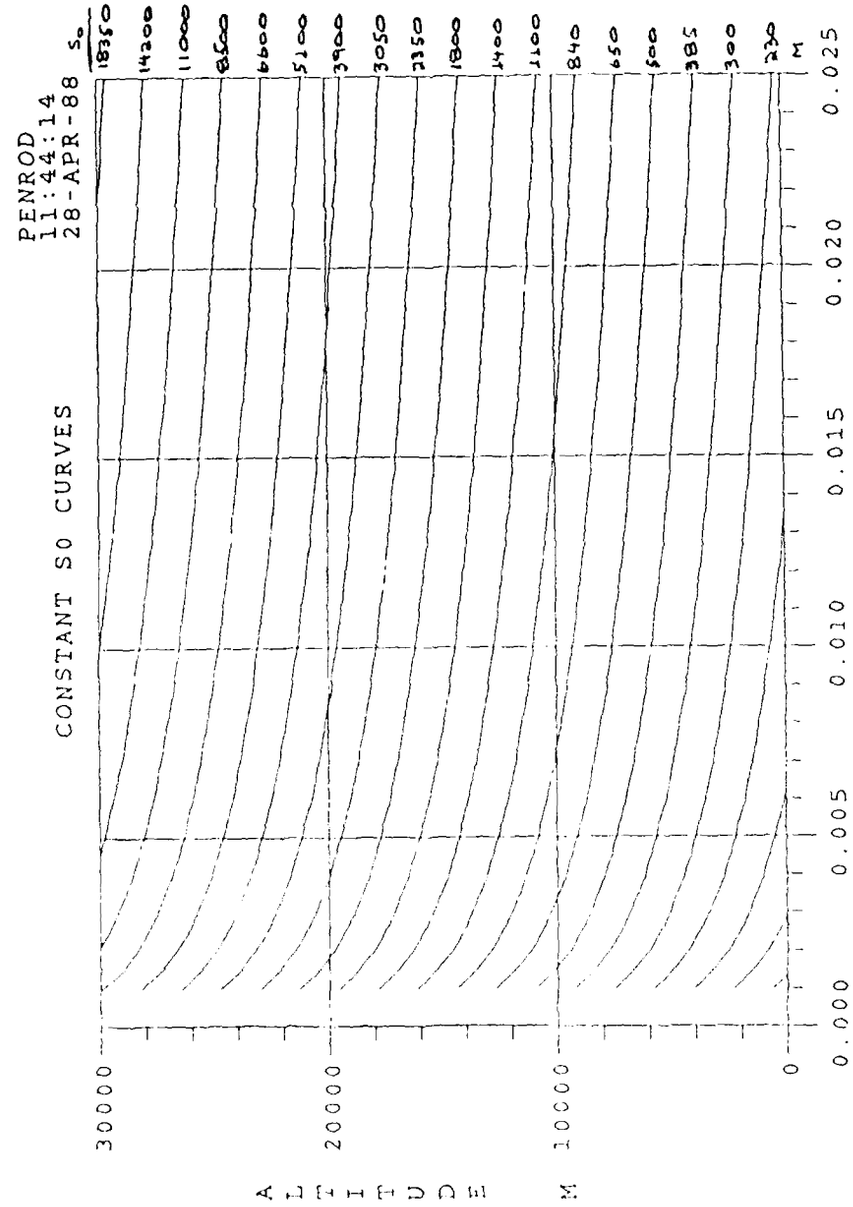

Figure 41. Drag Coefficient versus Altitude and Mass

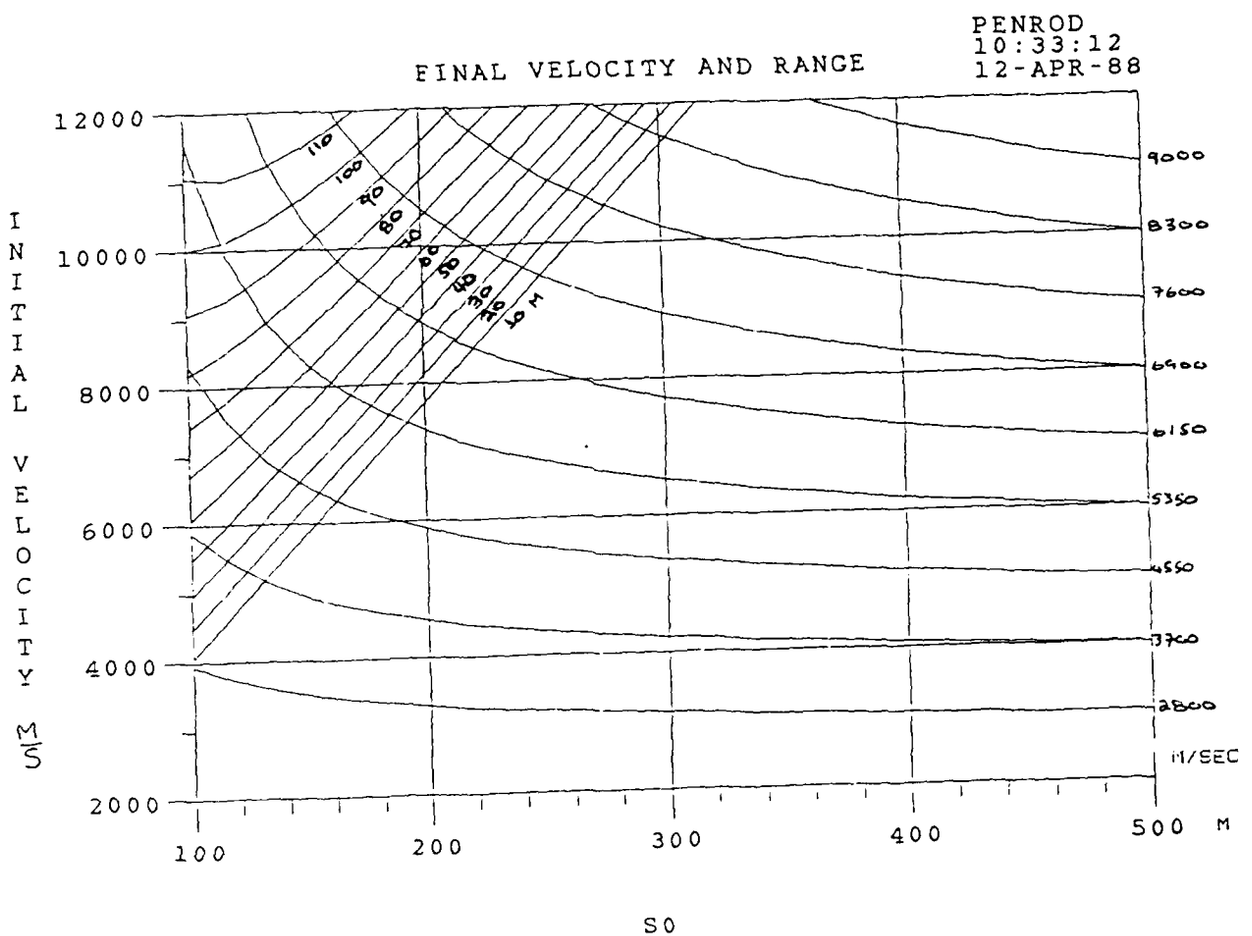

GRAPH A2. PELLET VELOCITY AND RANGE AT 0.01 SECONDS AFTER DETONATION

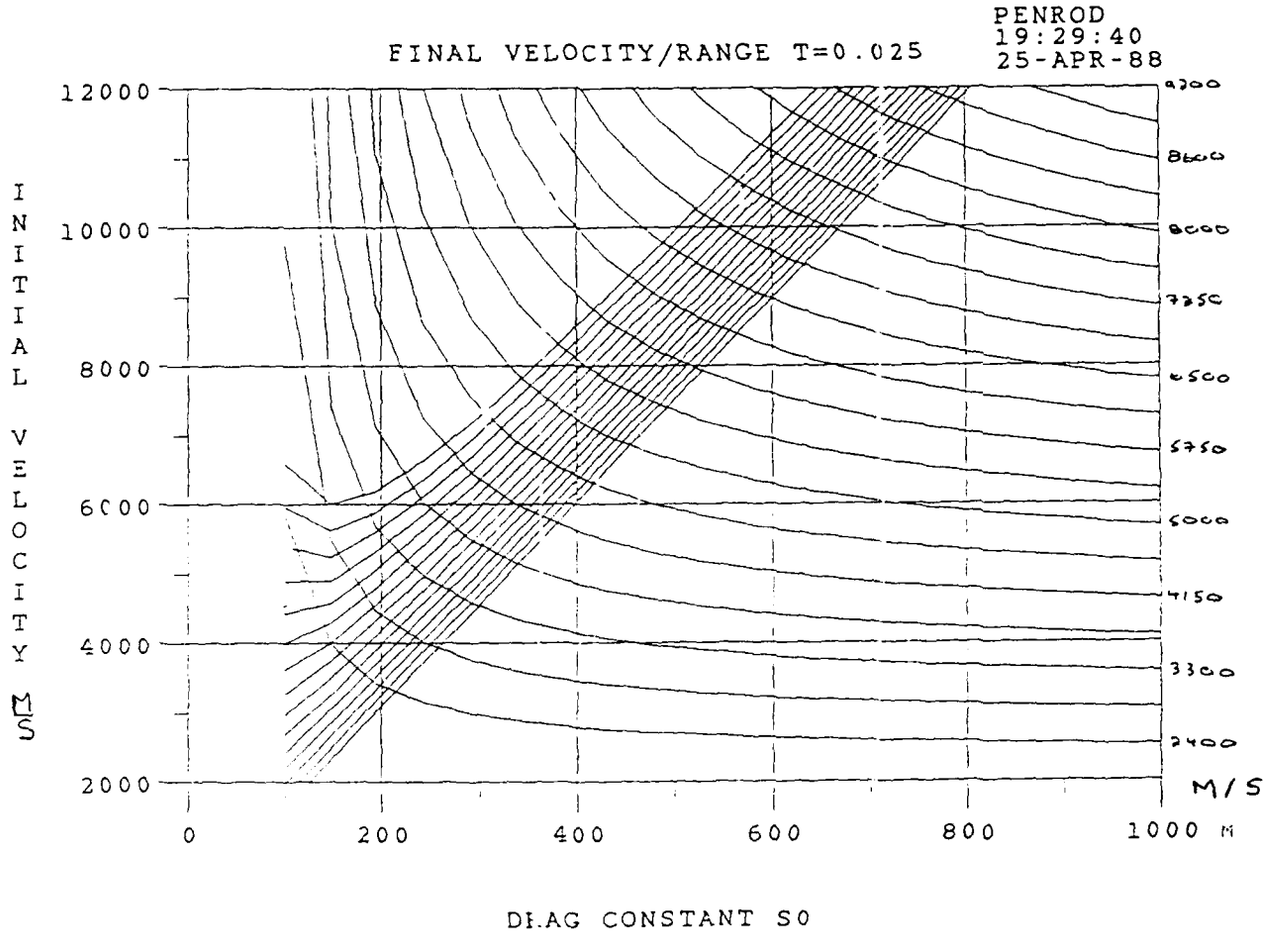

GRAPH #3. PELLET VELOCITY AND RANGE AT 0.025 SECONDS AFTER DETONATION

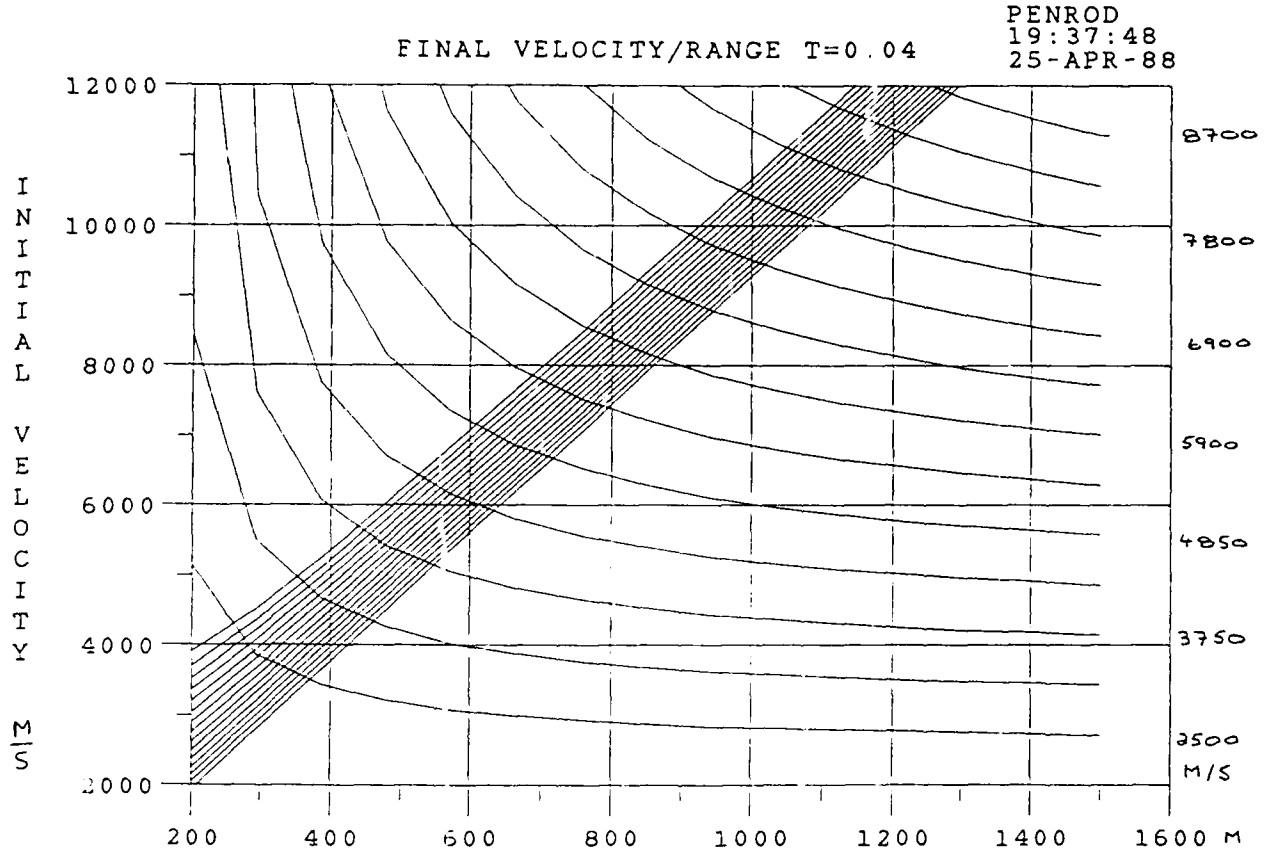

GRAPH A4. PELLET VELOCITY AND RANGE AT 0.04 SECONDS AFTER DETONATION

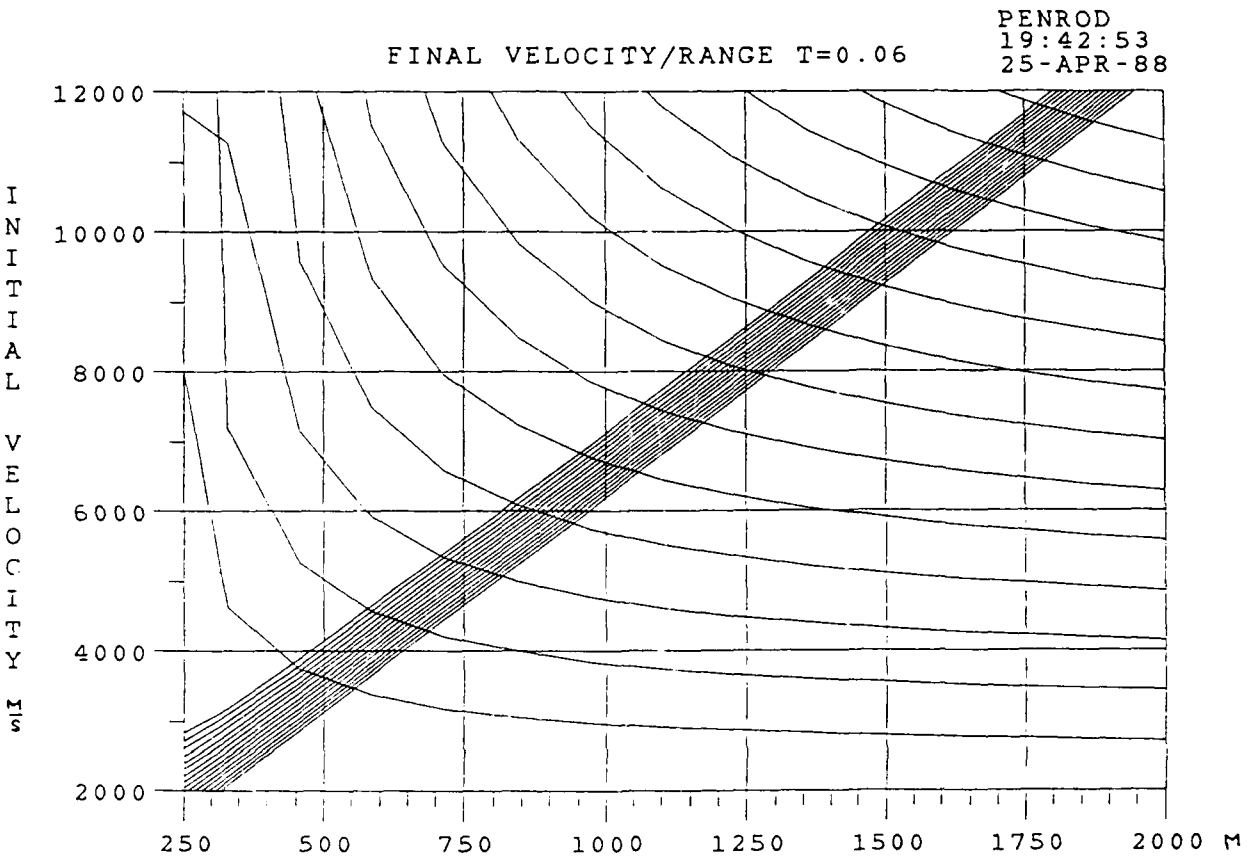

GRAPH A5. PELLET VELOCITY AND RANGE AT 0.06 SECONDS AFTER DETONATION

APPENDIX B. MISSILE DYNAMICS

Euler's general equations of motion for rigid bodies can be greatly simplified by placing the origin of the coordinate frame at the missile's center of gravity, as well as stipulating axial symmetry and a no roll condition, to yield:

$$\begin{aligned} \dot{u} &= A_x + rv - qw \\ \dot{v} &= A_y - ru \\ \dot{w} &= A_z - qu \\ L &= 0 \\ M &= I_y \dot{q} \\ N &= I_z \dot{r} \end{aligned} \qquad \text{(B-1)}$$

where u,v,w are the velocities and with a dot representing the velocity rates of change along the respective axes in the missile body (B) frame, A_X, A_Y, A_Z are the thrust and control accelerations, p,q,r are the roll, pitch ,yaw rates, L,M,N are the respective moments, and I_X, I_Y, I_Z are the respective inertias (Figure 6). Because the specific masses, inertias and control forces for this missile system are unknown at this stage of design, forces are generalized in terms of acceleration by taking advantage of the constant mass condition and force equation (a=F/m), while inertias and moments are ignored by defining rotational rates in terms of lateral acceleration and missile velocity:

$$p = 0$$
$$q = -A_z / u \qquad \text{(B-2)}$$
$$r = A_y / u$$

Translational velocity i the B frame is found by integrating the first three equations of (B-1). The missile's absolute motion in the inertial (I) frame can then be found by transforming the body velocity vector with a Direction Cosine Matrix (DCM) derived from the quaternions describing missile attitude (Appendix C). Position is solved for in a similar manner by integrating the velocity. Changes in missile attitude are determined by integrating rotation rates with respect to current heading. This study took advantage of the rarely used quaternion methods to evaluate these highly non-linear attitudinal differential equations.

APPENDIX C. QUATERNIONS

Quaternions, which were developed during the last century but which are only now coming into popular usage, utilize four parameters to uniquely characterize three dimensional orientation. The advantages to this method include simplified differential equations which avoid trigonometric functions, unique determination of any attitude without singularities, and a useful product rule to rotate through more than one coordinate system at a time. The one significant drawback is that individual parameters give no sense of physical orientation unlike Euler angles.

Quaternion parameters may be initialized in several ways. This study chose to use the Direction Cosine Matrix (DCM) which is easily derived from initial heading vectors:

$$DCM = \begin{bmatrix} a_{11} & a_{12} & a_{13} \\ a_{21} & a_{22} & a_{23} \\ a_{31} & a_{32} & a_{33} \end{bmatrix} = \begin{bmatrix} \hat{x}' \cdot \hat{x} & \hat{x}' \cdot \hat{y} & \hat{x}' \cdot \hat{z} \\ \hat{y}' \cdot \hat{x} & \hat{y}' \cdot \hat{y} & \hat{y}' \cdot \hat{z} \\ \hat{z}' \cdot \hat{x} & \hat{z}' \cdot \hat{y} & \hat{z}' \cdot \hat{z} \end{bmatrix} \quad \text{(C-1)}$$

where all axes are unit vectors and the primed terms represent the secondary coordinate system. The primary use of the DCM is in coordinate transformations which are

accomplished by multiplication:

$$\begin{bmatrix} x' \\ y' \\ z' \end{bmatrix} = \begin{bmatrix} \quad DCM \quad \end{bmatrix} \begin{bmatrix} x \\ y \\ z \end{bmatrix} \qquad \text{(C-2)}$$

where the primed values represent the vector's new components. Transformations in the reverse direction are easily done by inverting the DCM and multiplying. Since the DCM is an orthogonal matrix its inverse is merely the transpose of the DCM. Once the DCM has been calculated for the initial attitude, it is a simple matter to initialize the quaternion parameters:

$$\begin{aligned} q_4 &= \tfrac{1}{2}\sqrt{1 + a_{11} + a_{22} + a_{33}} \\ q_1 &= (a_{23} - a_{32}) / 4 q_4 \\ q_2 &= (a_{31} - a_{13}) / 4 q_4 \\ q_3 &= (a_{12} - a_{21}) / 4 q_4 \end{aligned} \qquad \text{(C-3)}$$

The main use of the quaternion then becomes to record orientation and to evaluate rates of attitudinal changes by integrating the rotational differential equations:

$$\begin{bmatrix} \dot{q}_1 \\ \dot{q}_2 \\ \dot{q}_3 \\ \dot{q}_4 \end{bmatrix} = \begin{bmatrix} q_4 & -q_3 & q_2 \\ q_3 & q_4 & -q_1 \\ -q_2 & q_1 & q_4 \\ -q_1 & -q_2 & -q_3 \end{bmatrix} \begin{bmatrix} p \\ q \\ r \end{bmatrix} \qquad \text{(C-4)}$$

where p,q,r are the rotation rates. Once the new orientation angles have been found a new DCM can be calculated:

$$\begin{bmatrix} q_1^2 - q_2^2 - q_3^2 + q_4^2 & 2(q_1 q_2 + q_3 q_4) & 2(q_1 q_3 - q_2 q_4) \\ 2(q_1 q_2 - q_3 q_4) & -q_1^2 + q_2^2 - q_3^2 + q_4^2 & 2(q_2 q_3 + q_1 q_4) \\ 2(q_1 q_3 + q_2 q_4) & 2(q_2 q_3 - q_1 q_4) & -q_1^2 - q_2^2 - q_3^2 + q_4^2 \end{bmatrix} \quad \text{(C-5)}$$

Euler angles can also be calculated from the quaternion to obtain an idea of actual compass direction:

$$\begin{aligned} \Theta &= \text{ARCSIN}\left[-2(q_1 q_3 - q_2 q_4)\right] \\ \Psi &= \text{ARCTAN}\left[\frac{2(q_1 q_2 + q_3 q_4)}{2(q_1^2 + q_4^2) - 1}\right] \\ \phi &= \text{ARCTAN}\left[\frac{2(q_2 q_3 + q_1 q_4)}{2(q_3^2 + q_4^2) - 1}\right] \end{aligned} \quad \text{(C-6)}$$

APPENDIX D. MISDYN COMPUTER SIMULATION CODE

```
_DJA2:[88.PENROD.TRIDENT.ACSL]MDCOM.CSL;2                    28-APR-

program INTERCEPT_SIMULATION_(MISDYN)

initial

'**********************INITIAL_ATTITUDE'
'DETERMINE INITIAL HEADING OF MISSILE, INITIALIZE QUATERNION'

        ARRAY           VMAIC(3),VMRIC(3),QNIC(4)

        CONSTANT        VMAIC = 0.0,0.0,-1.0 ...
                ,       VMRIC = 0.0,1.0,0.0

        CALL QUATERN(QNIC = VMAIC,VMRIC)

"**********************INITIAL_CONDITIONS"
'SET INITIAL VALUES FOR MISSILE AND TARGET VELOCITY AND POSITION'

        ARRAY           IMPIC(3),IMVIC(3),ITPIC(3),ITVIC(3),BMVIC(3),ITVDI(3)
        ARRAY           VBMAT(3,3),BVMAT(3,3)

        CONSTANT        IMPIC = 0.0,0.0,0.0 ...
                ,       IMVIC = 0.0,0.0,0.0 ...
                ,       ITPIC = 10000.0,10000.0,-10000.0 ...
                ,       ITVIC = -500.0,-500.0,250.0 ...
                ,       ITVDI = 3*1.0E-30

        CALL DCM(VBMAT,BVMAT = QNIC)
        CALL MULT(BMVIC = VBMAT,IMVIC)

'**********************GLOBAL_CONSTANTS'
'DEFINE CONSTANTS USED THROUGHOUT PROGRAM'

        CONSTANT        FUZE = 0.0, TFUZE = 0.0, TLFOM =0.0, ILFOM = 0.0
        CONSTANT        RMN = 1.0E-30, RMX = 1.0E30
        NSTEPS          NSTP = 1
        MAXTERVAL       MAXT = 0.002
        IALG    = 4
        PI      = ATAN2(0.,-1.)

end $'of initial'

dynamic

derivative

"**********************RELATIVE_GEOMETRY"
'CALCULATE RELATIVE GEOMETRY AND VELOCITY OF MISSILE'
'AND TARGET IN THE DIFFERENT FRAMES'

        ARRAY           IMP(3),IMV(3),ITP(3),ITV(3)
        ARRAY           VTP(3),VTRV(3),BTP(3),BTV(3),BTRV(3)
        ARRAY           QN(4),BMA(3)

        CONSTANT        BMA = 1.0,0.0,0.0

        CALL DCM(VBMAT,BVMAT = QN)

        CALL VECSUB(VTP  = ITP,IMP)
```

```
_DJA2:[88.PENROD.TRIDENT.ACSL]MDCOM.CSL;2                              28-APR-

        CALL VECSUB(VTRV = ITV,IMV)

        CALL MULT(BTP  = VBMAT,VTP)
        CALL MULT(BTV  = VBMAT,ITV)
        CALL MULT(BTRV = VBMAT,VTRV)

"************************SENSOR/FILTER"
'CALCULATE MEASUREMENTS THAT CAN BE DETERMINED BY SENSORS'

        ARRAY           CVVEL(3)

        RANGE = VECMAG(BTP)
        THETA = ANGLE(BMA,BTP)
        DTH   = DANGLE(BTP,BTRV)
        DRNG  = DOT(BTP,BTRV)/(VECMAG(BTP) + RMN)

        TTHE  = ANGLE(BTP,BTV)

        CALL NMACV(CVVEL = BTP,BTRV,BMV)

        PROCEDURAL(BTAZM = BTP)
            IF(BTP(2) .EQ. 0.0 .AND. BTP(3) .EQ. 0.0) BTP(3) = 1.0
            BTAZM = ATAN2(BTP(2),BTP(3))
        END $'OF PROCEDURAL'

'************************FUZING/WARHEAD'
'CHECKS IF CONDITIONS ARE OPTIMAL TO FIRE WARHEAD'

        CONSTANT        FURNG = 100.0, THFUZ = 0.08

        IF(THETA .LT. THFUZ .AND. RANGE .LT. FURNG) FUZE = RMX
        IF(FUZE .GT. 0.0 .AND. TFUZE .EQ. 0.0) TFUZE = T
        TFIRE = T - TFUZE

"************************GUIDANCE_LAW"
'IMPLEMENTS FOUR BASIC TYPES OF GUIDANCE LAWS'

        CONSTANT        PRED = 0.0, DVANG = 0.0, K1 = 1.0, ...
                        N = 4.0, BMALF = 0.0, ...
                        TBST = 0.5, TPURS =0.0, TTERM = 0.0, ...
                        MGLIM = 250.0, FLYPL = 0.0

        TEMP2 = VECMAG(BTV) / (VECMAG(BMV) + RMN) * SIN(TTHE)
        TEMP1 = RSW(ABS(TEMP2) .GT. 1.0, 1.0, TEMP2)
        LDANG = ABS(ASIN(TEMP1))
        CANG = RSW(PRED .EQ. 1.0, LDANG, DVANG)
        AC1 = K1 * VECMAG(BMV) * ABS(THETA - CANG)

        K2  = N * (VECMAG(BTRV)/(VECMAG(BMV)+RMN)) / (COS(LDANG)+RMN)
        AC2 = VECMAG(BMV)*K2*DTH

        ACC  = RSW(T .GE. TPURS, AC2, AC1)
        ACB  = RSW(T .GE. TBST, ACC, 0.0)
        AC   = BOUND(-MGLIM,ACB,MGLIM)

        CVY = RSW((PRED .EQ. 1.0) .OR. (T .GT. TPURS), ...
                                SIGN(CVVEL(2),BTP(2)), SIN(BTAZM))
        CVZ = RSW((PRED .EQ. 1.0) .OR. (T .GT. TPURS), ...
```

```
_DJA2:[88.PENROD.TRIDENT.ACSL]MDCOM.CSL;2                    28-APR-

                                SIGN(CVVEL(3),BTP(3)), COS(BTAZM))

        ACY = RSW(TGO .LT. TTERM, 0.0, AC * CVY)
        ACZ = RSW(TGO .LT. TTERM, 0.0, AC * CVZ)

"************************AERODYNAMIC_TRANSFER_FUNCTION"
'MODELS MISSILE DYNAMIC RESPONSE'

        ARRAY           NUM(2),DEN(3)
        CONSTANT        WN = 25.0, ZETA = 0.8, TAU = 2.0

        PROCEDURAL(NUM,DEN = WN,ZETA,TAU)
        NUM(1) = TAU * WN * WN
        NUM(2) = WN * WN
        DEN(1) = 1.
        DEN(2) = 2. * ZETA * WN
        DEN(3) = WN * WN
        END $'OF PROCEDURAL'

        R = TRAN(1,2,NUM,DEN, ACY/(VECMAG(BMV)+RMN))
        Q = TRAN(1,2,NUM,DEN,-ACZ/(VECMAG(BMV)+RMN))

        RV = LEDLAG(0.0,TAU,R,0.0)
        QV = LEDLAG(0.0,TAU,Q,0.0)

        AY = VECMAG(BMV) * RV
        AZ = VECMAG(BMV) *-QV

"************************TRANSLATIONAL_KINEMATICS"
'CALCULATES MISSILE ACCELERATION, VELOCITY, POSITION'

        ARRAY           BMVD(3),BMV(3),IMPD(3),TBMV(3),TIMV(3)
        CONSTANT        AT = 250.0, MVLIM = 1500.0

        AX = RSW(VECMAG(BMV) .LT. MVLIM, AT, 0.0)

        PROCEDURAL(BMVD=AX,ACY,ACZ,BMV,R,Q,FUZE)
            BMVD(1) = RSW(FUZE .GT. 0.0, 0.0, AX + R*BMV(2) - Q*BMV(3))
            BMVD(2) = RSW(FUZE .GT. 0.0, 0.0, AY - R*BMV(1))
            BMVD(3) = RSW(FUZE .GT. 0.0, 0.0, AZ + Q*BMV(1))
        END $'OF PROCEDURAL'

        BMV = INTVC(BMVD,BMVIC)

        ALF  = ATAN((BMV(2)**2+BMV(3)**2)/(VECMAG(BMV)+RMN))
        ALFA = ATAN(BMV(3)/(BMV(1)+RMN))
        ALFB = ATAN(BMV(2)/(VECMAG(BMV)+RMN))

        CALL TRVEL(TBMV = BMV)
        CALL MULT(TIMV = BVMAT,TBMV)

        CALL MULT(IMV = BVMAT,BMV)

        PROCEDURAL(IMPD = IMV,FUZE)
            IMPD(1) = RSW(FUZE .GT. 0.0, 0.0, IMV(1))
            IMPD(2) = RSW(FUZE .GT. 0.0, 0.0, IMV(2))
            IMPD(3) = RSW(FUZE .GT. 0.0, 0.0, IMV(3))
        END $'OF PROCEDURAL'
```

```
      IMP = INTVC(IMPD,IMPIC)

"************************ROTATIONAL_KINEMATICS"
'CALCULATES NEW ATTITUDE OF MISSILE'

      ARRAY          QND(4),QNA(4)
      CONSTANT       P = 0.0

      PA=RSW(FUZE .GT. 0.0, PA, P)
      QA=RSW(FUZE .GT. 0.0, QA, Q)
      RA=RSW(FUZE .GT. 0.0, RA, R)

      CALL DQUATERN(QND = QN,PA,QA,RA)

      QNA = INTVC(QND,QNIC)
      CALL NORM(QN = QNA)

"************************TARGET_MOTION"
'CALCULATES TARGET MOTION'

      ARRAY          ITPD(3),ITVD(3),TITPD(3)

      CALL XFERB(ITVD = ITVDI,3)
      ITV = INTVC(ITVD,ITVIC)

      CALL VECSUB(TITPD = ITV,TIMV)

      PROCEDURAL(ITPD = ITV,TITPD,FUZE)
          ITPD(1) = RSW(FUZE .GT. 0.0, TITPD(1), ITV(1))
          ITPD(2) = RSW(FUZE .GT. 0.0, TITPD(2), ITV(2))
          ITPD(3) = RSW(FUZE .GT. 0.0, TITPD(3), ITV(3))
      END $'OF PROCEDURAL'

      ITP = INTVC(ITPD,ITPIC)

end $'of derivative'

'************************LETHALITY'
'CALCULATES LETHALITY FIGURE OF MERIT'

      ARRAY          VFRAG(3)
      CONSTANT       NUMFR = 1000.0, MFRAG = 0.001, RHOFR = 19800.0, ...
                     CD = 0.92, BDIA = 0.2, TAREA = 0.5, ...
                     THDEV = 0.08, PDVFR = 0.05, VFIRE = 5000.0

      VFRAG(1) = VFIRE
      VFRAG(2) = BMV(1)
      VFRAG(3) = VFIRE + BMV(1)

      ALT = -IMP(3)

      RHOATMO = 1.752*EXP(-ALT/6700.)
      SO = 2./(DATMO*CD)*(MFRAG/PI)**(1./3.)*(4./3.*RHOFR)**(2./3.)

      IF((FUZE .GT. 0.0) .AND. (THETA .LT. THDEV)) ...
              CALL DRAGFOM(ILFOM = TAREA,SO,NUMFR,MFRAG, ...
                           BDIA,THDEV,PDVFR,BTP,BTV,VFRAG,TFIRE,CINT)
```

```
      TLFOM = TLFOM + ILFOM

'************************TIME'

      CONSTANT        CINTZ = 0.01, TGOMN = 2.0E-4, TSTP = 10.0, ...
                      TFLTMN = 0.0, CINTMN = 0.001

      TGO1 = (-DOT(BTP,BTRV) + RMN)/((VECMAG(BTRV) **2) + RMN)
      TGO  = RSW(FUZE .GT. 0.0, 0.1, TGO1)
      CINT = RSW(FUZE .GT. 0.0, CINTMN, AMAX1(CINTMN,AMIN1(ABS(TGO),CINTZ)))
      TERMT(T.GE.TSTP .OR. (TGO1.LE.TGOMN .AND. T.GE.TFLTMN) ...
                              .OR. (TLFOM .GT. 0.0 .AND. ILFOM .EQ. 0.0))

'************************EULER_ANGLES'
'CALCULATE EULER ANGLES FOR SENSE OF MISSILE ATTITUDE'

      ATHE = 180.*ASIN(-2.*(QN(1)*QN(3)-QN(2)*QN(4)))/PI
      APSI = 180.*ATAN2(2.*(QN(1)*QN(2)+QN(3)*QN(4)),...
                        2.*(QN(1)**2+QN(4)**2)-1.)/PI
      APHI = 180.*ATAN2(2.*(QN(2)*QN(3)+QN(1)*QN(4)),...
                        2.*(QN(3)**2+QN(4)**2)-1.)/PI

end $'of dynamic'
end $'of program'
      SUBROUTINE QUATERN(X,Y,QN)
C     INITIALIZES QUATERNION FROM DIRECTION COSINE MATRIX'

      REAL X(3),Y(3),Z(3),QN(4)

      CALL UNIT(X,X)

      IF (VECMAG(Y) .EQ. 0.0) THEN
          IF (X(1) .EQ. 0.0) THEN
              Y(1)=SIGN(1.,X(2))
              Y(2)=0.0
          ELSE IF (X(2) .EQ. 0.0) THEN
              Y(1)=0.0
              Y(2)=SIGN(1.,X(1))
          ELSE
              Y(1)=-1./X(1)
              Y(2)= 1./X(2)
          END IF
          Y(3)=0.0
      END IF
      CALL UNIT(Y,Y)

      CALL CROSS(X,Y,Z)
      CALL UNIT(Z,Z)

      QN(4)=SQRT(1.+X(1)+Y(2)+Z(3))/2.
      QN(1)=(Y(3)-Z(2))/(4.*QN(4))
      QN(2)=(Z(1)-X(3))/(4.*QN(4))
      QN(3)=(X(2)-Y(1))/(4.*QN(4))

      RETURN
      END
```

```
      SUBROUTINE DQUATERN(QN,P,Q,R,QND)
C     CALCULATES QUATERNION DERIVATIVES

      REAL QN(4),QND(4),P,Q,R

          QND(1) = ( QN(4)*P - QN(3)*Q + QN(2)*R)/2.
          QND(2) = ( QN(3)*P + QN(4)*Q - QN(1)*R)/2.
          QND(3) = (-QN(2)*P + QN(1)*Q + QN(4)*R)/2.
          QND(4) = (-QN(1)*P - QN(2)*Q - QN(3)*R)/2.

      RETURN
      END


      SUBROUTINE DCM(QN,A,INVA)
C     PRODUCES A DIRECTION COSINE MATRIX FROM QUATERNION

      REAL QN(4),A(3,3),INVA(3,3)

      A(1,1) =  QN(1)**2 - QN(2)**2 - QN(3)**2 + QN(4)**2
      A(1,2) = 2.*(QN(1)*QN(2) + QN(3)*QN(4))
      A(1,3) = 2.*(QN(1)*QN(3) - QN(2)*QN(4))
      A(2,1) = 2.*(QN(1)*QN(2) - QN(3)*QN(4))
      A(2,2) = -QN(1)**2 + QN(2)**2 - QN(3)**2 + QN(4)**2
      A(2,3) = 2.*(QN(2)*QN(3) + QN(1)*QN(4))
      A(3,1) = 2.*(QN(1)*QN(3) + QN(2)*QN(4))
      A(3,2) = 2.*(QN(2)*QN(3) - QN(1)*QN(4))
      A(3,3) = -QN(1)**2 - QN(2)**2 + QN(3)**2 + QN(4)**2

      INVA(1,1) = A(1,1)
      INVA(1,2) = A(2,1)
      INVA(1,3) = A(3,1)
      INVA(2,1) = A(1,2)
      INVA(2,2) = A(2,2)
      INVA(2,3) = A(3,2)
      INVA(3,1) = A(1,3)
      INVA(3,2) = A(2,3)
      INVA(3,3) = A(3,3)

      RETURN
      END

C*****************************************************
C     UTILITY PROGRAMS

      SUBROUTINE VECSUB(X,Y,Z)
C     SUBTRACTS TWO VECTORS

      REAL X(3),Y(3),Z(3)

      DO 10 I=1,3
         Z(I) = X(I) - Y(I)
10    CONTINUE

      RETURN
      END
```

```
      SUBROUTINE MULT(MAT,VECIN,VECOUT)
C     MULTIPLIES MATRIX BY A VECTOR

      REAL MAT(3,3),VECIN(3),VECOUT(3),SUM
      INTEGER I,J

      DO 10 I=1,3
          SUM = 0.0
          DO 20 J=1,3
              SUM = SUM + MAT(I,J)*VECIN(J)
20        CONTINUE
          VECOUT(I) = SUM
10    CONTINUE

      RETURN
      END


      FUNCTION VECMAG(X)
C     CALCULATES MAGNITUDE OF VECTOR

      REAL VECMAG,X(3)

      VECMAG = SQRT(DOT(X,X))

      RETURN
      END


      FUNCTION DOT(X,Y)
C     EVALUATES VECTOR DOT PRODUCT

      REAL DOT,X(3),Y(3)

      DOT = X(1)*Y(1) + X(2)*Y(2) + X(3)*Y(3)

      RETURN
      END


      SUBROUTINE CROSS(X,Y,Z)
C     EVALUATES VECTOR CROSS PRODUCT
      REAL X(3),Y(3),Z(3)

      Z(1) = X(2)*Y(3) - Y(2)*X(3)
      Z(2) = X(3)*Y(1) - Y(3)*X(1)
      Z(3) = X(1)*Y(2) - Y(1)*X(2)

      RETURN
      END


      SUBROUTINE UNIT(X,Y)
C     FINDS THE UNIT VECTOR OF A VECTOR

      REAL X(3),Y(3),NORM
```

```
      NORM = VECMAG(X)

      DO 10 I=1,3
         Y(I) = X(I) / (NORM + 1.E-30)
10    CONTINUE

      RETURN
      END


      FUNCTION ANGLE(X,Y)
C     FINDS ANGLE FORMED BY TWO VECTORS

      REAL ANGLE,X(3),Y(3)

      TEMP = DOT(X,Y)/(VECMAG(X)*VECMAG(Y) + 1.E-30)
      IF (ABS(TEMP) .GT. 1.0) TEMP = 1.0
      ANGLE = ABS( ACOS( TEMP ) )

      RETURN
      END


      FUNCTION DANGLE(P,V)
C     CALCULATES ANGULAR RATE OF CHANGE

      REAL P(3),V(3),TEMP1,TEMP2

      RMN = 1E-30

      TEMP1 = P(1)*((P(2)*V(2)+P(3)*V(3))/(SQRT(P(2)**2+P(3)**2)+RMN))
      TEMP2 = V(1)*SQRT(P(2)**2+P(3)**2)

      DANGLE = (TEMP1 - TEMP2) / (P(1)**2 + P(2)**2 + P(3)**2 + RMN)

      RETURN
      END


      SUBROUTINE NMACV(RPOS,RVEL,VEL,CVEC)
C     CALCULATES DIRECTION OF NORMAL ACCELERATION VECTOR

      REAL RPOS(3),RVEL(3),CVEC(3),RMN,VEL(3),FP(3)
      INTEGER I

      RMN = 1.0E-30

      CALL CROSS(RVEL,RPOS,FP)
      CALL CROSS(VEL,FP,CVEC)
      CALL UNIT(CVEC,CVEC)

      RETURN
      END


      SUBROUTINE NORM(IN,OUT)
C     NORMALIZES QUATERNIONS
```

```
_DJA2:[88.PENROD.TRIDENT.ACSL]MDCOM.CSL;2                              28-APR-

      REAL IN(4),OUT(4),MAG,SUMMAG
      INTEGER I

      SUMMAG = 0
      DO 10 I = 1,4
         SUMMAG = IN(I) * IN(I) + SUMMAG
10    CONTINUE
      MAG = SQRT(SUMMAG)

      DO 20 I=1,4
          OUT(I) = IN(I) / (MAG + 1.E-30)
20    CONTINUE

      RETURN
      END

      SUBROUTINE TRVEL(BMV,TBMV)
C     REDEFINES RELATIVE VELOCITY AFTER DETONATION

      REAL BMV(3),TBMV(3)

      TBMV(1) = 0.0
      TBMV(2) = BMV(2)
      TBMV(3) = BMV(3)

      RETURN
      END

C*************************************************************************
C     LETHALITY MODELS

      SUBROUTINE DRAGFOM(TA,SO,NF,MF,BD,TH,DV,RP,TV,VF,T,DT,LETHFOM)
C     CALCULATES LETHALITY FIGURE OF MERIT OVER AN INTERVAL

      REAL RP(3),TV(3),VF(3)
      REAL TA,NF,MF,DF,CD,BD,TH,DV,ALT
      REAL RV(3),STDDEV(3),INTERV(3),P(3),HIBOUND(3),LOBOUND(3),MNCO(3)
      REAL VFI,RHOATMO,SO,RANGE,VHI,VLO
      REAL PI,MININT,PROBSF,VOLOFINT,MEANDENS,N,VIMPACT,LETHFOM
      INTEGER I

      PI = ATAN2(0.,-1.)

      RANGE = VECMAG(RP)
      VFI = VFINI(RANGE,SO,T)

      IF (ABS((VFI - VF(3))/VF(3)) .GT. DV ) THEN
             LETHFOM = 0.0
             GOTO 999
      ENDIF

      RV(1) = TV(1) - VFFIN(VFI,SO,T)
      RV(2) = TV(2)
      RV(3) = TV(3)

      STDDEV(1) = DV*VF(3)/3.
      STDDEV(2) = (TH*RP(1) + BD)/6.
      STDDEV(3) = (TH*RP(1) + BD)/6.
```

```
      MININT = SQRT(2.*TA)

      MNCO(1) = SQRT(RV(2)**2/(RV(1)**2+RV(2)**2))
      MNCO(2) = SQRT(RV(1)**2/(RV(1)**2+RV(2)**2))
      MNCO(3) = SQRT((RV(1)**2+RV(2)**2)/(VECMAG(RV)**2))

      DO 10 I=1,3
          INTERV(I)  = ABS(TV(I)*DT) + MNCO(I)*MININT
          HIBOUND(I) = RP(I) + INTERV(I)/2.
          LOBOUND(I) = RP(I) - INTERV(I)/2.
10    CONTINUE

      VHI = VFINI(HIBOUND(1),SO,T-DT/2.) - VF(3)
      VLO = VFINI(LOBOUND(1),SO,T+DT/2.) - VF(3)

      CALL NORMPDF(P(1),STDDEV(1),VHI,VLO)

      DO 20 I=2,3
          CALL NORMPDF(P(I),STDDEV(I),HIBOUND(I),LOBOUND(I))
20    CONTINUE

      PROBSF = P(1)*P(2)*P(3)
      VOLOFINT = INTERV(1)*INTERV(2)*INTERV(3)
      MEANDENS = PROBSF*NF/VOLOFINT
      N=MEANDENS*TA*VECMAG(TV)*DT
      VIMPACT = VECMAG(RV)
      LETHFOM = N*MF*VIMPACT*VIMPACT/(2.*SQRT(TA))

999   CONTINUE

      RETURN
      END


      FUNCTION VFINI(R,SO,T)
C     CALCULATES INITIAL VELOCITY OF PELLET FRAGMENT FROM RANGE

      REAL VFINI,R,SO,T

      VFINI = SO/(T + 1.E-30) * EXP(R/SO-1.)

      RETURN
      END


      FUNCTION VFFIN(V0,SO,T)
C     CALCULATES FINAL VELOCITY OF PELLET FRAGMENT FROM INITIAL VELOCITY

      REAL VFFIN,V0,SO,T

      VFFIN = (V0*SO) / (V0*T+SO)

      RETURN
      END

      SUBROUTINE NORMPDF(NORMPROB,SIGMA,HI,LO)
C     CALCULATES VALUE OF NORMAL DISTRIBUTION BETWEEN TWO BOUNDS
```

_DJA2:[88.PENROD.TRIDENT.ACSL]MDCOM.CSL;2 28-APR-

```
      REAL NORMPROB,SIGMA,HI,LO
      REAL PI,INTERV,DELTA,T,F(0:21),SUM,PART
      INTEGER I,N,N1

      PI = ATAN2(0.,-1.)

      INTERV = HI - LO
      N = 20
      DELTA = INTERV/N

      DO 100 I=0,N
          T = (LO + I*DELTA)/SIGMA
          F(I) = (1./(SIGMA*SQRT(2.*PI)))*EXP(-T*T/2.)
100   CONTINUE

      SUM = 0
      DO 200 I=0,(N-2),2
          PART = F(I) + 4.*F(I+1) + F(I+2)
          SUM = SUM + PART
200   CONTINUE

      NORMPROB = (DELTA/3.)*SUM

      RETURN
      END
```